ASL-TR-0046

AD

Reports Control Symbol
OSD 1366

FOG EVOLUTION IN THE VISIBLE AND INFRARED SPECTRAL REGIONS AND ITS MEANING IN OPTICAL MODELING

DECEMBER 1979

By
Richard D.H. Low

Approved for public release; distribution unlimited

US Army Electronics Research and Development Command
ATMOSPHERIC SCIENCES LABORATORY
White Sands Missile Range, NM 88002

NOTICES

Disclaimers

The findings in this report are not to be construed as an official Department of the Army position, unless so designated by other authorized documents.

The citation of trade names and names of manufacturers in this report is not to be construed as official Government indorsement or approval of commercial products or services referenced herein.

Disposition

Destory this report when it is no longer needed. Do not return it to the originator.

SECURITY CLASSIFICATION OF THIS PAGE (When Date Entered)

ERADCOM/ REPORT DOCUMENTATION PAGE		READ INSTRUCTIONS BEFORE COMPLETING FORM
1. REPORT NUMBER ASL-TR-0046	2. GOVT ACCESSION NO.	3. RECIPIENT'S CATALOG NUMBER
4. TITLE (and Subtitle) FOG EVOLUTION IN THE VISIBLE AND INFRARED SPECTRAL REGIONS AND ITS MEANING IN OPTICAL MODELING		5. TYPE OF REPORT & PERIOD COVERED R&D Technical Report
		6. PERFORMING ORG. REPORT NUMBER
7. AUTHOR(s) Richard D. H. Low		8. CONTRACT OR GRANT NUMBER(s)
9. PERFORMING ORGANIZATION NAME AND ADDRESS Atmospheric Sciences Laboratory White Sands Missile Range, New Mexico 88002		10. PROGRAM ELEMENT, PROJECT, TASK AREA & WORK UNIT NUMBERS DA Task No. 1L161101AH 71
11. CONTROLLING OFFICE NAME AND ADDRESS US Army Electronics Research and Development Command Adelphi, MD 20783		12. REPORT DATE December 1979
		13. NUMBER OF PAGES 40
14. MONITORING AGENCY NAME & ADDRESS (if different from Controlling Office)		15. SECURITY CLASS. (of this report) UNCLASSIFIED
		15a. DECLASSIFICATION/DOWNGRADING SCHEDULE

16. DISTRIBUTION STATEMENT (of this Report)

Approved for public release; distribution unlimited.

17. DISTRIBUTION STATEMENT (of the abstract entered in Block 20, if different from Report)

18. SUPPLEMENTARY NOTES

19. KEY WORDS (Continue on reverse side if necessary and identify by block number)

Fog microphysics	Models
Evolution	Germany
Visible	California
Infrared	

20. ABSTRACT (Continue on reverse side if necessary and identify by block number)

For the first time in the field of cloud physics, high-density fog drop-size data from the time near fog formation through the time near fog dissipation became available at 5-minute intervals from field measurements carried out at Meppen, Germany, on 3-4 March 1978. The fog was believed to have been brought about by frontal passage. Extinction coefficients in the 0.55μm, 3.80μm, and 10.6μm spectral regions were calculated from the measured drop-size distributions and plotted as a function of time to depict optical evolution of the fog. Such spectral evolution in relation to fog microphysical evolution was examined in

CONT

DD FORM 1 JAN 73 1473 EDITION OF 1 NOV 65 IS OBSOLETE

SECURITY CLASSIFICATION OF THIS PAGE (When Date Entered)

40 663

20. ABSTRACT (cont)

detail to attempt to formulate optical models or scaling laws for electro-optical sensors applications. A cursory comparison was made with the California advection and radiation-advection fogs observed at Fort Ord on 3 and 9 May 1978, respectively, because the available data portrayed only portions of their life cycles. Because of their low liquid water contents and high number concentration, the haze regimes in these fogs played a dominant role in "messing up" spectral transmission in the 0.55μm and 3.80μm regions, usually during the phase of fog formation.

Multispectral extinction coefficients appeared to delineate a fog's life history better than microphysical parameters. Five models or scaling laws relating liquid water content to extinction in the three wavelength regions are presented: one for each of the three fogs, one for their pooled data, and one for the two California fogs together. Regression analysis indicated that the three fogs were significantly different from one another as would be expected in the sense that they belonged in different types. The correlation coefficients of extinction versus liquid water content in these models varied from 0.95 to 0.99. Further inspection of those data points used in deriving regression lines showed that in the 3.80μm region the models might be more appropriately represented by a quadratic fit in logarithmic space. Since the linear fit was nearly perfect in the 10.6μm region, design of an instrument using this feature was suggested.

In the final analysis, the choice of a particular or a general model or scaling law should be dictated by the sensitivities and requirements of the electro-optical sensors to be deployed.

CONTENTS

1. INTRODUCTION

Sensor systems, weapons direction systems, and communication systems which depend upon the propagation of optical infrared wavelength energy through the atmosphere are being developed and employed. Solutions to critical problems in system design, deployment, and overall utility are paced by knowledge and understanding of atmospheric effects on energy transmission according to the Department of Defense (DOD) plan for atmospheric transmission research and development, 16 March 1978, approved by the Under Secretary of Defense. The plan showed that aerosols such as fogs, hazes, smokes, dusts, clouds, and other randomly distributed atmospheric particles are poorly understood, and it was recommended that a capability be developed to measure, model, and predict accurately the atmospheric transmission effects of such naturally occurring aerosols.

Of these various naturally occurring atmospheric aerosols, fog may stand out as the one which would have the most serious effect on the operations of the Army's electro-optical weapons and communication systems owing to its persistence and intensity. Fog data have been collected and studied since the beginning of the century.[1] More recent fog data may be found in a large number of papers and reports cited in Houghton and Radford[2] and Stewart.[3] Despite their relative abundance, these fog data are judged to be inadequate for modeling atmospheric transmission in different spectral regions. Low et al[3],[4] have discussed fog data deficiencies. New fog data are needed which extend measurements of particle sizes to tenths of a micrometer in diameter and which are more accurately characterized in terms of the prevailing synoptic situation and the dominant mechanism that causes fog formation.

During February and March 1978, the Atmospheric Sciences Laboratory made meteorological and microphysical measurements in Meppen, Germany. Except for brief spells of clearing, light snow, drizzle, haze and fog occurred almost persistently from 13 February through 5 March 1978 when the field measurements ended. Despite persistent haze and fog occurrences, the

[1]H. G. Houghton and W. H. Radford, 1938, "On the Measurement of Drop-Size and Liquid Water Content in Fogs and Clouds," Papers in Physical Oceanography and Meteorology, Vol VI, No 4

[2]D. A. Stewart, 1977, "Infrared and Submillimeter Extinction by Fog," Technical Report TR-77-9, Technology Laboratory, Physical Science Directorate, Redstone Arsenal, AL

[3]Richard D. H. Low, Louis D. Duncan, and Richard B. Gomez, 1978, "The Microphysical Basis of Fog Optical Characterization," ASL-TR-0011, US Army Atmospheric Sciences Laboratory, ERADCOM, White Sands Missile Range, NM

[4]Richard D. H. Low, Louis D. Duncan, and Y. Y. Roger R. Hsiao, 1979, "Microphysical and Optical Properties of California Coastal Fogs at Fort Ord," ASL-TR-0034, US Army Atmospheric Sciences Laboratory, ERADCOM, White Sands Missile Range, NM

record of fog and haze data is fragmentary and so is the record of surface observations, except for the period of 3 to 4 March 1978. A complete documentation of the Meppen field measurement program on instrumentation, geography, topography, weather analysis, data collection procedure, and particulate data will be published later.[5]

A detailed spectral analysis is covered in this report for the fog period of 3 to 4 March 1978. By careful examination and comparison of temporal variations of both the optical and microphysical properties of these fogs from formation through dissipation, insight may be gained in the complex nature of fog and haze optical modeling; then the diversity of the various models could be explained and a more logical judgment arrived at as to the quality of one model versus another for different fogs, individually or collectively. The two Fort Ord fogs were selected for comparison, some aspects of which have been investigated.[4] This study was limited to the spectral regions of 0.55μm, 3.80μm, and 10.6μm wavelengths and the derived liquid water content used as the common parameter in establishing models.

The following section briefly discusses the nature of the microphysical data 3 to 4 March 1978, and the treatment of the data are given. In section 3, the temporal variations of the extinction coefficients in the three spectral regions are examined, and such spectral variations are interpreted in the light of microphysical factors. Then regression relationships between spectral attenuation and liquid water content in these wavelength regions are established together with a statistical analysis of these regression lines or scaling laws. Microphysical implications in optical modeling are discussed in section 4. In the final section, the findings together with certain conclusions are summarized.

2. DATA PROCESSING

Fog drop-size samples were taken in the Meppen fog of 3 to 4 March about every 30 seconds by a Knollenberg particle counter, model FSSP-100C,* which covers a size range of 0.25μm to 23μm radius. Some 8 to 10 samples were averaged by size categories to produce data points every 5 minutes. Fog particle data were collected from 1828 hours LST, 3 March through 1100

[5]J. D. Lindberg, 1979, Private communications

[4]Richard D. H. Low, Louis D. Duncan, and Y. Y. Roger R. Hsiao, 1979, "Microphysical and Optical Properties of California Coastal Fogs at Fort Ord," ASL-TR-0034, US Army Atmospheric Sciences Laboratory, ERADCOM, White Sands Missile Range, NM

*Questions were raised by Pinnick and Auvermann (1979, "Response Characteristics of Knollenberg Light-Scattering Aerosol Counters," J Aerosol Sci, 10:55-74) about the definition of its manufacturer's size ranges. Unfortunately, the authors fail to provide their calibration values.

hours LST, 4 March (about 170 data points at 5-minute intervals). Actually, light rain, light drizzle, and ground fogs had been reported almost all day prior to the sampling time. Nevertheless, the fog did not begin to thicken until about 2200 hours. Following the termination of measurements at 1100 hours, the fog still persisted in patches for another 8 hours or so and was then followed again by light drizzle and rain, though the fog was no longer as thick as it had been. Unfortunately, the entire life history of this fog was not completely captured, but the data recorded was sufficient to delineate the fog evolution reasonably well, especially in comparison with the Fort Ord fog data. The 3 and 9 May 1978 Fort Ord fogs were of the advection and radiation-advection types, respectively, The Meppen fog was of the frontal type.

Once a drop-size distribution is given, its volume extinction coefficient can be easily obtained by the following formula:

$$\beta(\lambda) = \pi \int_{r_o}^{r_x} r^2 \, Q(m,r,\lambda) n(r) \, dr \, , \qquad (1)$$

where $\beta(\lambda)$ is the total volume extinction coefficient per unit length at a wavelength λ; $Q(m,r,\lambda)$ the extinction efficiency factor, a function of wavelength, complex refractive index m, and particle radius r; and $n(r)$ the number density or concentration of droplets from radius r to r + dr.

The integration interval for equation (1) is from r_o, the smallest droplet radius, to r_x, the largest droplet. The total liquid water content per unit volume is given by

$$W = \frac{4}{3} \pi \rho_o \int_{r_o}^{r_x} r^3 \, n(r) \, dr \, , \qquad (2)$$

where ρ is the density of a droplet, taken to be unity in the case of fog, and W is the liquid water content. Furthermore, one is often interested

in the percentage contribution that a size interval makes to spectral attenuation. The expression for calculating percentage spectral contributions is shown below:

$$F(r_i,\lambda) = \frac{\int_{r_i}^{r_o} Q(m,r,\lambda)\, r^2\, n(r)\, dr}{\int_{r_o}^{r_x} Q(m,r,\lambda)\, r^2\, n(r)\, dr}, \qquad (3)$$

where r_i is any droplet radius less than or equal to r_x, and $F(r_i,\lambda)$ is the cumulative percentage contribution.

With the data processed according to equations (1) to (3), it was possible to generate different kinds of plots to facilitate analysis.

3. OPTICAL AND MICROPHYSICAL PROPERTIES

Each fog has a life of its own.[6,7,8,9] No two fogs at two different places look exactly alike, meteorologically, microphysically, or environmentally; however, all fogs would have to go through a life cycle of formation, growth, maturity, and dissipation on the basis of microphysical considerations. The fog life cycle can also be examined in the light of its optical evolution. In this way, one would gain a better understanding not only of how a fog evolves spectrally throughout its entire life but also, more importantly, of why sometimes one single model or scaling law may not completely represent that fog or any other one.

---

[6]Richard D. H. Low, 1975, "Microphysical Evolution of Fog," J Research Atmosphere, 2:23-32

[7]R. J. Pilié, E. J. Mack, W. C. Kocmond, W. J. Eadie, and C. W. Rogers, 1975, "The Life Cycle of Valley Fogs: Part II: Fog Microphysics," J Appl Meteorol, 14:364-374

[8]W. T. Roach, R. Brown, S. J. Caughly, J. A. Garland, and C. J. Readings, 1976, "The Physics of Radiation Fogs: Ia-Field Study," Quart J Roy Meteorol Soc, 102:313-333

[9]J. Goodman, 1977, "The Microstructure of California Coastal Fog and Stratus," J Appl Meteorol, 16:1056-1067

3.1 Spectral Evolution

Figure 1 (a and b) depicts the spectral evolution of the Meppen fog at 0.55μm, 3.80μm, and 10.60μm wavelengths. The bold lines on the abscissa show the time periods where the fog drop-size spectra are presented; these periods were chosen because the fog appeared to have gone through some dramatic changes in its life.

If a freehand trend line were drawn from about 1830 to about 0114 hours when the fog reached its peak growth spectrally, the line would appear to slope upward. Then the line would begin to stabilize but show a gentle, downward trend. By about 1000 hours, the fog would display a tendency to dissipate, although it would not. Tenuous as it may be on the basis of cloud physics considerations, the international definition that fog has a visibility of 1 km or less may be used, which is nearly equivalent to an extinction coefficient of 4 km^{-1} or greater in the visible. The period from 1830 through 2217 hours in which the visibility remained above 1 km may be regarded as representing the formation stage of the fog, where it was observed to be rather inhomogeneous in its structure. During this phase, each extinction coefficient followed its own course of evolution. In terms of transmission, the 10.60μm region was the best and the visible the worst, with the 3.80μm lying in between. By about 2217 hours as the fog began to grow vigorously, the extinction coefficients in these three wavelength regions closed in upon one another, and the 3.80μm coefficient then climbed above the visible and stayed up there until near dissipation. The period from about 2217 through about 0114 hours may be looked upon as the growth phase during which the fog showed appreciable homogeneity. From 0114 hours on, the fog appeared to become stabilized despite fluctuations due to the usual atmospheric turbulence and may be said to have reached the mature stage, which lasted for about 9 hours. During this period, the fog became quite homogeneous. The aging fog did not disappear for another 8 hours when it was apparently washed out by a light rain.

The spectral evolution of the Fort Ord advection fog of 3 May 1978 is shown in figure 2 and that of the Fort Ord radiation-advection fog of 9 May in figure 3. In neither case can the life history be clearly traced. Except for greatly reduced attenuation and the period up to about 0130 hours, the 3 May fog appeared to resemble the mature phase of the Meppen fog. The fog had already formed somewhere over the ocean as a low-hanging stratus cloud and reached some aspect of maturity before the cloud drifted onshore with the sea breeze. The fog data for the period up to 0130 hours could very well represent the leading edge of the incoming stratus. The figure does not show clearly which phase of life of the 9 May morning fog is being depicted. Judging from the clustering of the three extinction coefficients, one might suspect that the fog grew and stabilized in a great hurry before being burned off by the rising sun. In any case, these two fogs were fairly homogeneous.

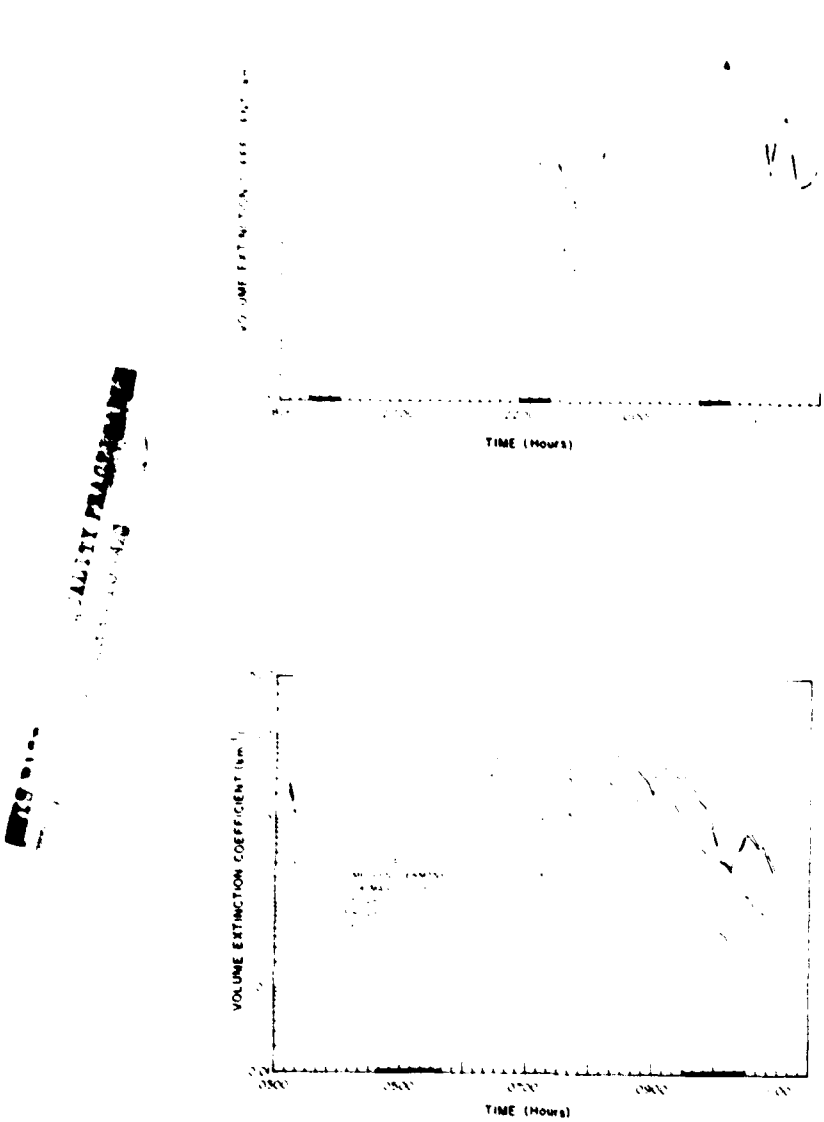

Figure 1 (a and b). Fog evolution in three spectral regions, Meppen, Germany, 3-4 March 1978.

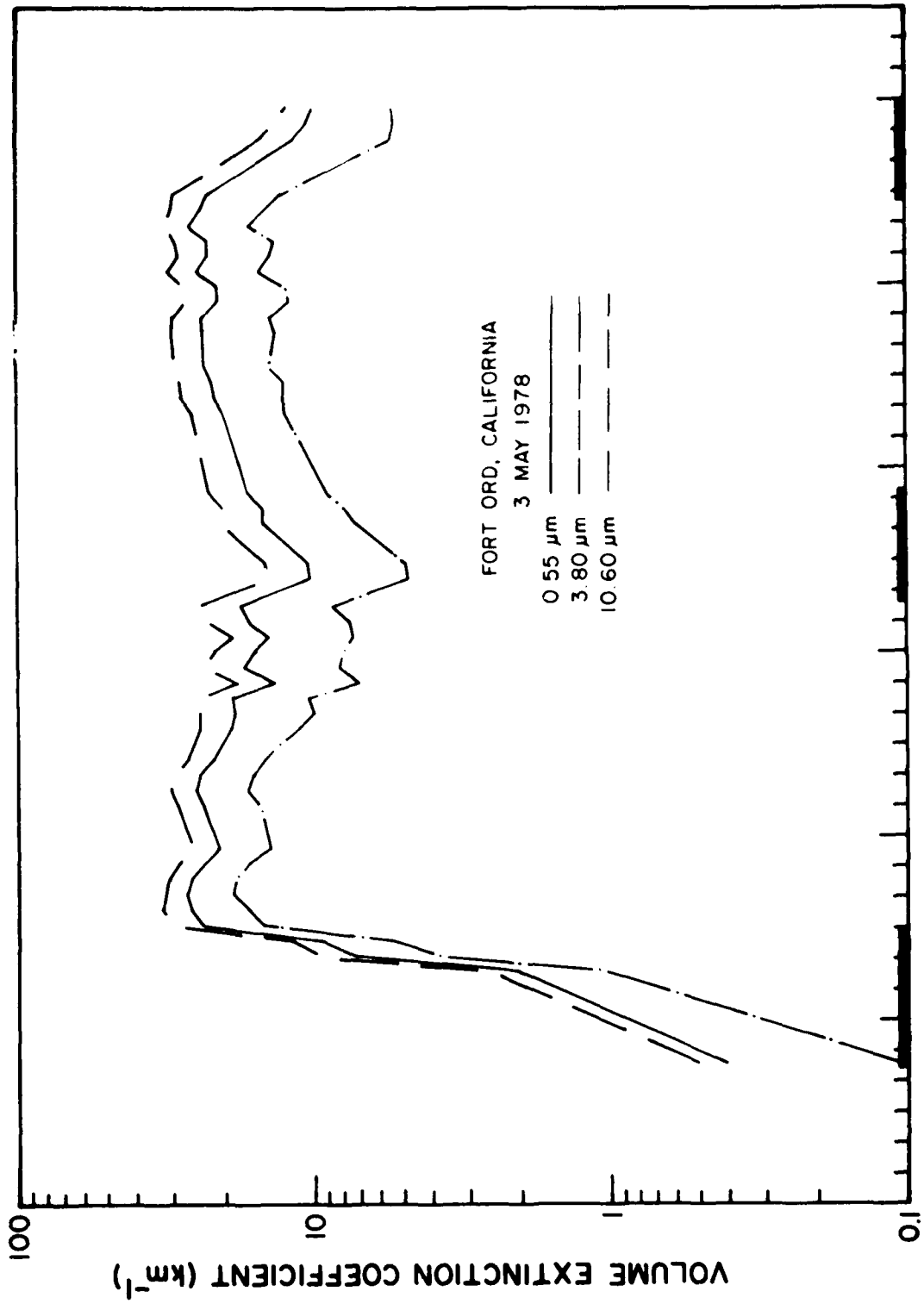

Figure 2. Fog evolution in three spectral regions, Fort Ord, California, 3 May 1978.

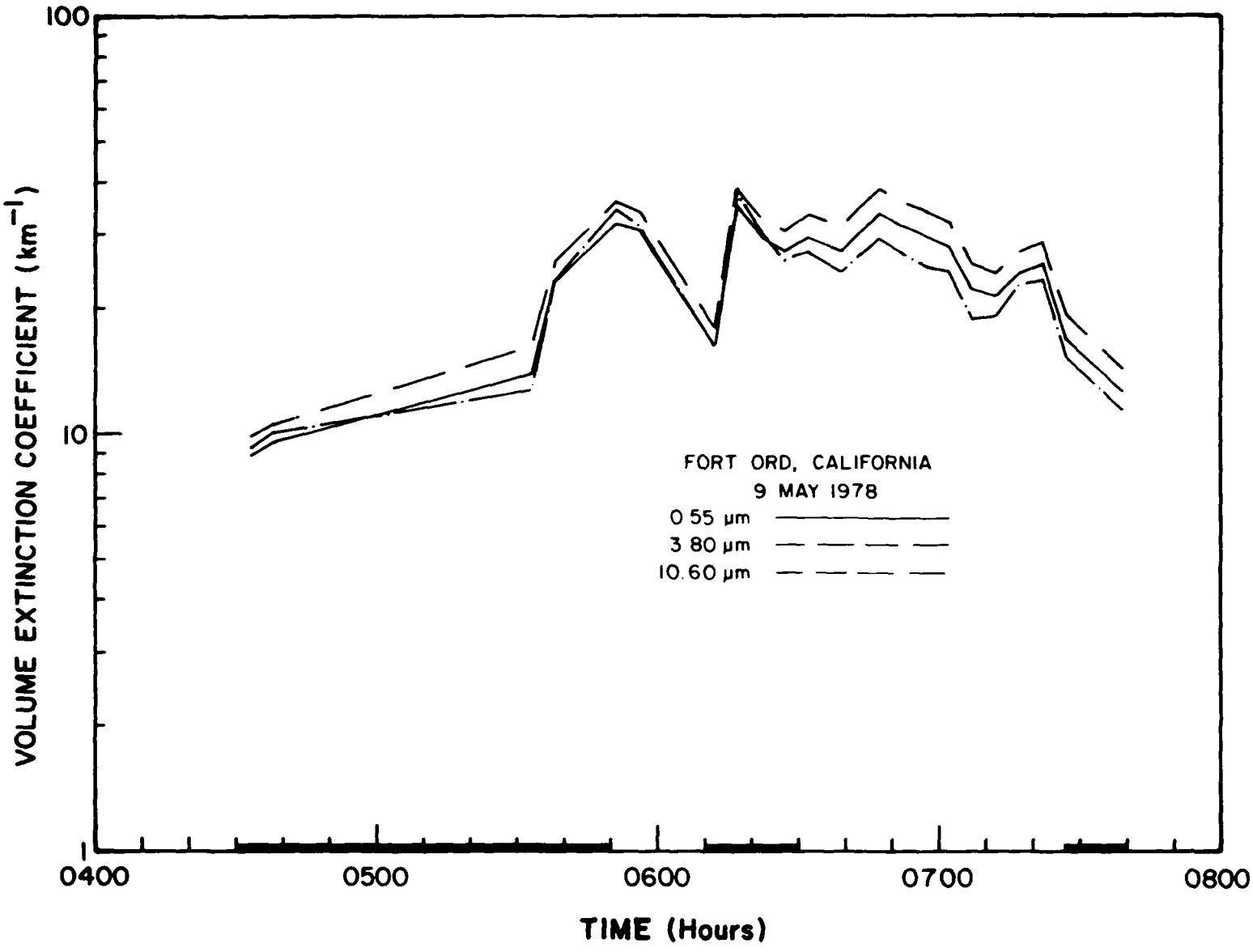

Figure 3. Fog evolution in three spectral regions, Fort Ord, California, 9 May 1978.

Fog spectral evolution will now be examined in terms of application. Let the contrast threshold be taken in the visible at 5 percent instead of the usual 2 percent. Assume that the electro-optical sensors can recognize a target also at the 5 percent level in the infrared (which is probably conservative, considering the almost certain contamination of sensor optics in such a hazy and foggy environment in addition to the sensor's inherent electronics noise level). Further assume that the sighting distance must be at least 500 meters for a missile to accomplish its final course adjustment. Then a line can be drawn across those graphs from the 6 km^{-1} point in the ordinate. These fogs would render any sensors in these wavelength ranges completely ineffective, except for short periods during their formation phase and perhaps also during their dissipation phase. However, if the required minimum sighting range is reduced to 100 meters, only the sensors in the 10.6μm region would be capable of operating most of the time in the Meppen fog, but in the Fort Ord fogs the sensors in the other spectral regions can operate as well. The reason for this can be found only by studying fog microphysics.

3.2 Spectral Evolution versus Drop-Size Distribution

The relationship between optical evolution and drop-size distribution in terms of size range and the magnitude of the haze regime will be examined. Figure 4 (a through e) illustrates the evolution of drop-size distributions in the Meppen fog for periods during which dramatic changes appeared to have taken place. Although incomplete, the drop-size spectra of the Fort Ord fogs on 3 and 9 May are depicted for comparison in figure 5 (a through c) and figure 6 (a through c), respectively. In each time period, which may span from 30 to 60 minutes, three drop-size distribution curves are presented. In this way, some idea of how drop-size spectra had evolved during each period and how they affected attenuation may be gained. The approximate time at which the dramatic change presumably occurred is shown. The number concentrations, size ranges, and mode radii of the spectra have been extracted from the graphs by estimation. While there is usually only one mode in the haze regime,[10,11] there may be one or more in the fog sector. However, only the first one was picked. The others would be useful in studying the microphysical processes of collision, coalescence, sedimentation, and turbulence. With the addition of liquid water content, the above-mentioned parameters are summarized in table 1.

[10] E. E. Hindman II, and O. E. R. Heimdahl, 1977, "Submicron Haze Droplets and Their Influence on Visibility in Fog," Preprints: 6th Conference on Inadvertent and Planned Weather Modification, American Meteorological Society, Boston, 10-13

[11] Richard D. H. Low, Louis D. Duncan, and Y. Y. Roger R. Hsiao, 1979, "Microphysical and Optical Properties of California Coastal Fogs at Fort Ord," ASL-TR-0034, US Army Atmospheric Sciences Laboratory, ERADCOM, White Sands Missile Range, NM

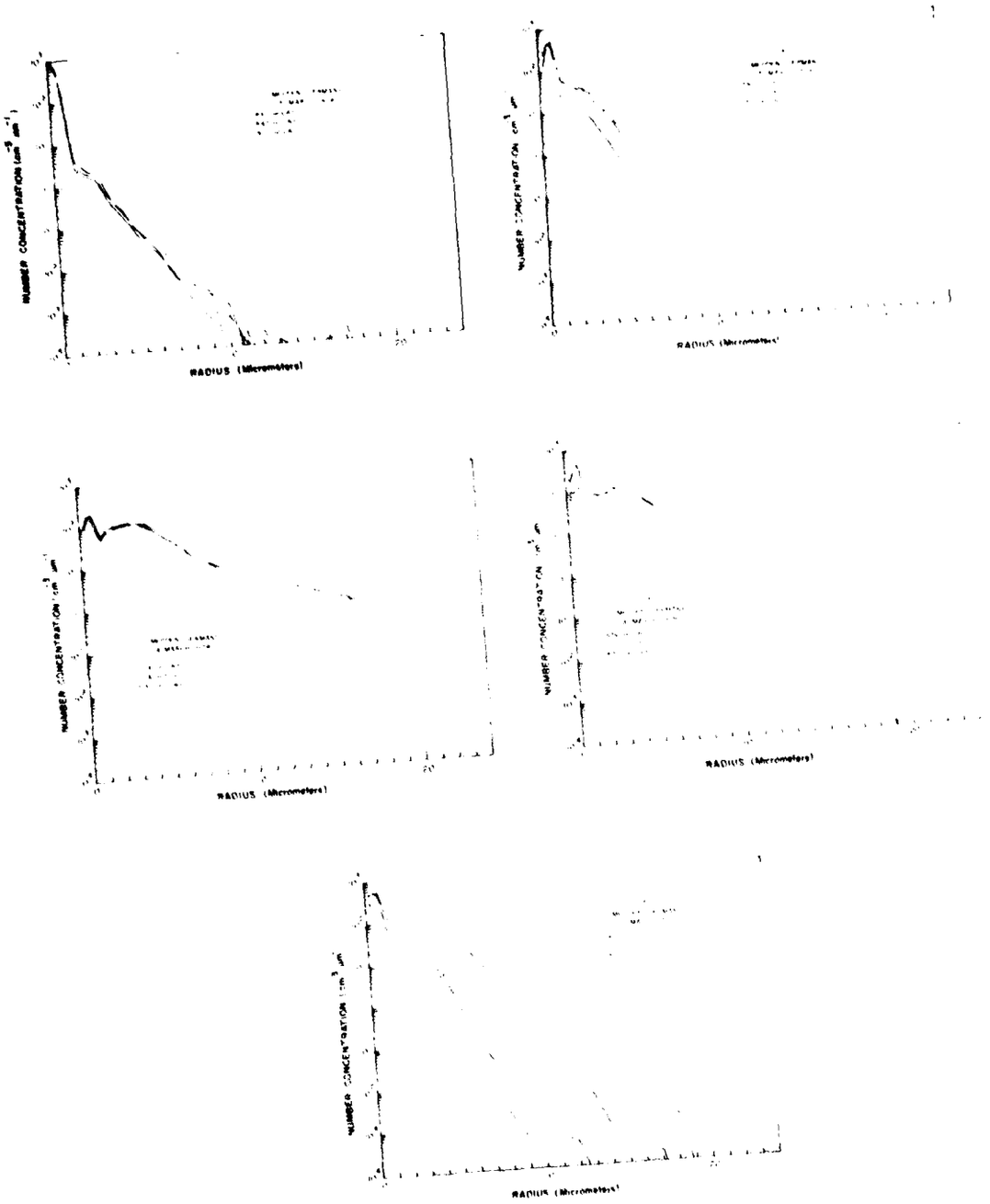

Figure 4 (a through e). Fog drop-size evolution for periods marked in figure 1 (a and b), Meppen, Germany, 3-4 March 1978.

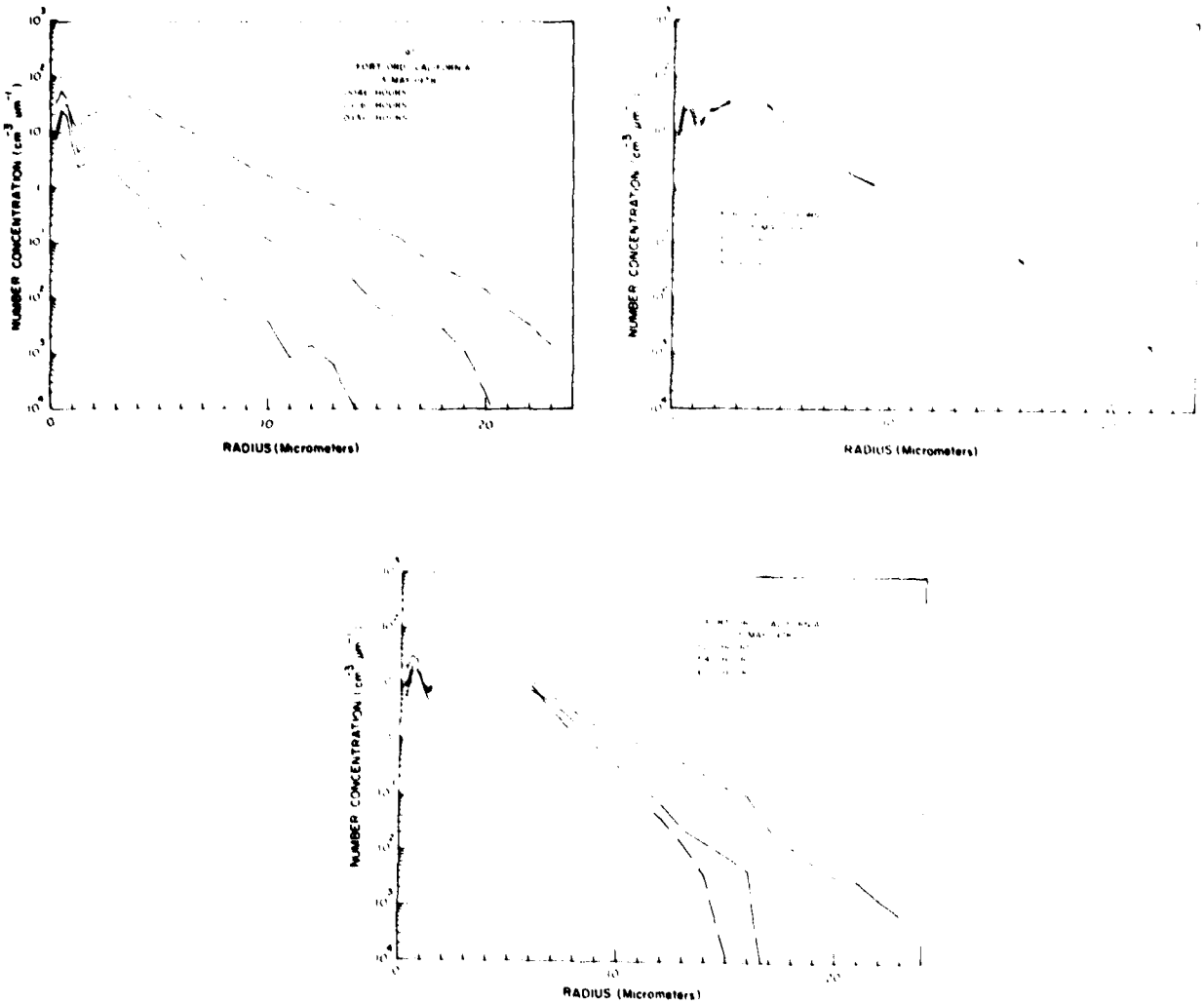

Figure 5 (a through c). Fog drop-size evolution for periods marked in figure 2, Fort Ord, California, 3 May 1978.

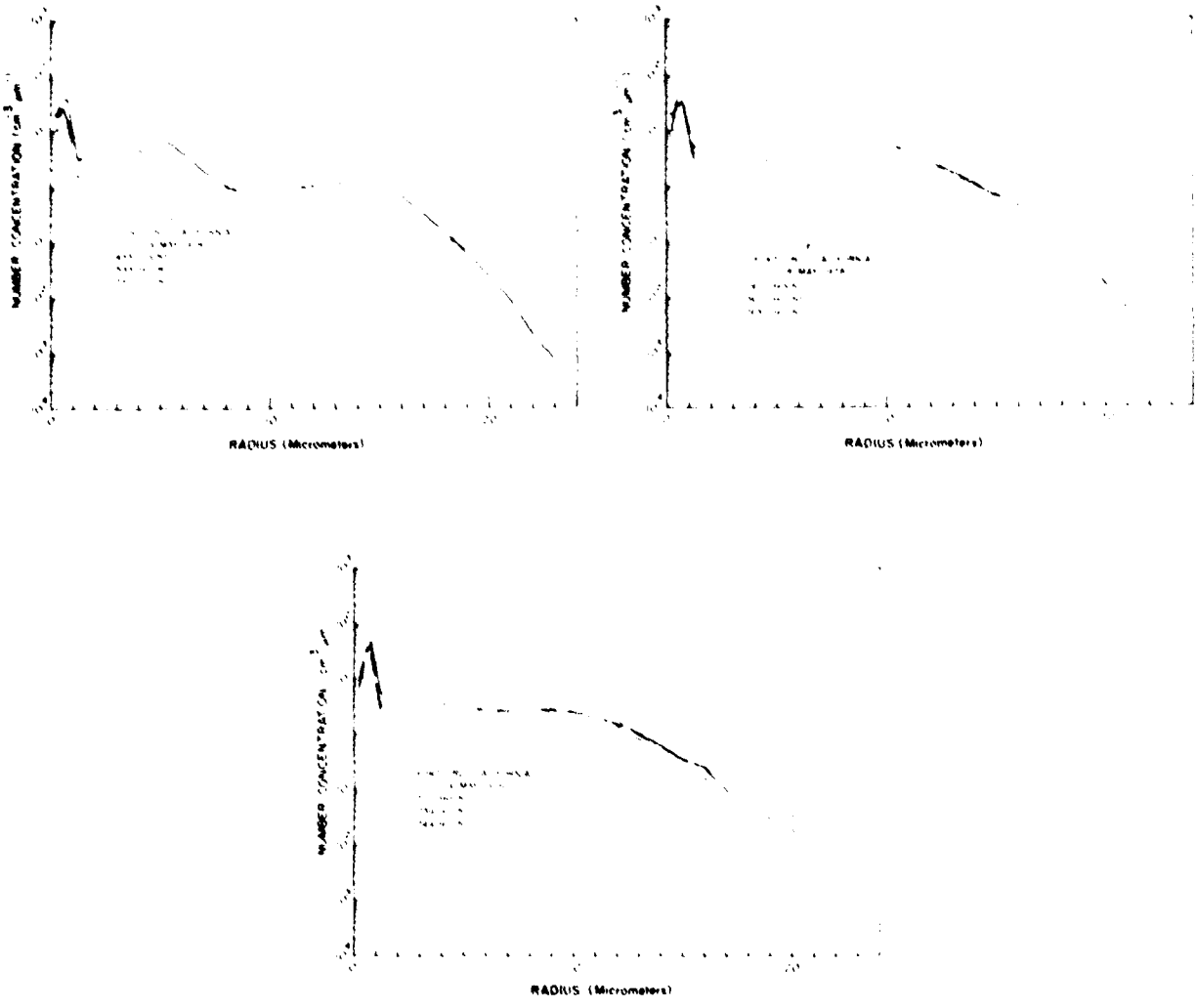

Figure 6 (a through c). Fog drop-size evolution for periods marked in figure 3, Fort Ord, California, 9 May 1978.

TABLE 1. TEMPORAL VARIATIONS OF MODE RADII, NUMBER DENSITY, LIQUID CONTENT, AND SIZE RANGE

Time	First Mode r(μm)	First Mode n(cm^{-3} μm^{-1})	Second Mode r(μm)	Second Mode n(cm^{-3} μm^{-1})	Total Liquid Water Content (mg m^{-3})	Size Range (μm)
			Meppen, Germany, 3-4 March 1978			
1832	0.25	800	2.40	14	0.382	0.25-10.7*
2217	0.40	500	2.40	35	22.80	0.25-**
0114	0.50	200	3.00	100	280.80	0.25-**
0539	0.50	130	3.50	90	160.30	0.25-20.5*
1000	0.40	550	2.70	40	4.15	0.25-12.5*
			Fort Ord, California, 3 May 1978			
0046	0.40	25	2.40	3	0.793	0.25-14.0*
0329	0.40	30	3.40	35	33.60	0.25-20.3*
0547	0.40	20	3.40	30	36.30	0.25-15.0*
			Fort Ord, California, 9 May 1978			
0433	0.40	25	3.90	3	67.90	0.25-**
0622	0.40	40	3.50	5	217.70	0.25-**
0744	0.50	35	4.00	4	88.06	0.25-**

*Number densities dropped below 10^{-4} cm^{-3}.

**At 23μm radius, the instrument limit, the number density is greater than 10^{-2} cm^{-3}.

The figures in relation to spectral evolution shall be discussed. During the early formation period the three extinction coefficients differed appreciably (figure 1a). Two features were dominant (figure 4a): a large haze regime (in comparison with the fog part) and a small size range. As a result, there was little water in the fog during this period. The number concentration of the first mode was nearly 60 times that of the second. Note in figure 1a that the infrared extinctions at 10.6μm and 3.80μm were nearly 18 and 4 times, respectively, lower than those in the visible. When the 3.80μm extinction curve crossed the 0.55μm curve (figure 1a), the haze regime (figure 4b) shrunk considerably, and the drop-size range of the fog regime extended beyond the sampling limit of the Knollenberg particle counter; as a result, there was an appreciable increase in liquid water content. Now the number concentration of the first mode dropped to 14 times that of the second. In neither case could a similar pattern of evolution be found in the Fort Ord fogs.

The Meppen fog then went through a period of rapid growth. By the time the three extinction coefficients approached one another (figure 1a), microphysical evolution (figure 4c) almost stopped (cf. figures 5b and 6c) during this period. The fog appeared to have attained its maximum growth at about 0114 hours. Its liquid water content jumped to 280.8 mg m^{-3}, and the number ratio of the first mode to the second dropped to 2. The haze regime became insignificant, and the drop-size range went far beyond the instrument's sizing capability. Neither of the Fort Ord fogs reached such intensity in terms of liquid water and attenuation. From then on, the fog began to stabilize and was on its downward excursion (figure 1b), neglecting the turbulent fluctuations. These fluctuations, which could be taken as an indication of turbulent mixing, are necessary to promote a fog's growth in depth and sustain its life[11] and often bring about homogeneity. Figure 4d shows that the haze regime became appreciable again, and the size range dropped to about 20μm radius. During the period from about 0300 through 0930 hours, the three extinction coefficients maintained their separate paces in an orderly manner with the 3.80μm coefficient staying on top of the other two. Although stable and mature, the fog began to age, and the microphysical mechanism of sedimentation took its toll of large droplets (figure 4e). Turbulent mixing appeared to have subsided but worked to dissipate the fog as the temperature rose in its diurnal march. Figures 1b and 4e show that the two extinction coefficients in the 0.55μm and the 3.80μm wavelength regions met again and stayed close together (compare the period from 2158 to 2232 hours) but the drop-size distribution curves (figure 4b and 4e) were entirely different. The haze regime had somewhat regained its former magnitude. The 3 May Fort Ord fog, as noted earlier, resembled the Meppen fog in the

[11]B. Rodhe, 1962, "The Effect of Turbulence on Fog Formation," Tellus, 14:49-86

latter's stable and mature phase (cf. figures 1b and 2) and appeared to dissipate near the end of the sampling period during which the evolution of its drop-size spectra in figure 5c bore some resemblance to that of figure 4e. However, the 9 May fog still looked rather stable near the end of drop-size measurement.

The Meppen fog was dealt with in great detail, while the Fort Ord fogs played a minor role. In summarizing, an interesting but puzzling observation was that despite their variations the mode radii in both regimes in these fogs were nearly of the same size, whereas the magnitudes of their haze regimes were quite different. Except for the formation period of the Meppen fog, the shapes of their haze regimes looked alike, yet the number density of the mode radius in the Meppen fog was at least one order of magnitude greater than that in the Fort Ord fogs. The magnitudes of the haze regimes in the latter were quite comparable even though they belonged in different fog types and had vastly different liquid water contents. Moreover, the number concentration of the mode radius in the fog regime of the Meppen fog never once caught up with that of its haze sector. Only when the fog was about to attain its peak growth did the ratio of their number reach a minimum. In the 3 May advection fog, the two modes often exchanged their positions in number concentrations, but the second mode on the average appeared to have the upper hand. The 9 May radiation-advection fog resembled the Meppen fog, if limited to comparing their haze and fog regimes.

This phenomenon may be briefly interpreted from a microphysical point of view. The air over Meppen was relatively rich in submicron particles, most likely a result of pollution, many of which would serve as fog condensation nuclei. By contrast, the air over Fort Ord was relatively clean but rich in large sea-salt particles which grow easily and can attain great sizes in a short time under slight supersaturation. In fact, the haze regime in the 3 May fog could have been picked up while the low-hanging stratus was moving overland; this may account for the similar haze regimes in the two Fort Ord fogs. Another noteworthy feature in these fogs is that the extinction curves with the 3.80μm wavelength on top, the 0.55μm wavelength in the middle, and the 10.6μm wavelength at the bottom, which appeared to be normal in a fog when its visible extinction went beyond 3 km^{-1} (or 1 km visibility at the 5 percent contrast threshold). Note that the crossover of the 0.55μm and the 3.80μm curves in the Meppen fog took place at about 1 km visibility, as shown in figure 1a at 2217 hours. An indication that visible extinction may not correlate well with 3.80μm extinction, except for certain segments of the fog's life, is a problem that will be examined further.

3.3 Microphysical Factors in Spectral Attenuation

The above discussion essentially dealt with how drop-size evolution was reflected in spectral evolution, or vice versa. In this part a few

individual drop-size spectra will be examined and an attempt made to find the factors that brought about spectral extinction as it was. Figure 7 (a through e) was prepared to depict five normalized cumulative distributions of the Meppen fog at about 4-hour intervals through the fog's life cycle. Two cumulative distributions each of the Fort Ord fogs are shown for comparison in figure 8 (a and b) and figure 9 (a and b). After some consideration, the median radius of a distribution, which can be readily estimated from the figures, was felt to be as meaningful as any other parameter such as mean volume radius or root-mean-square radius in explaining spectral attenuation. In the same vein, the "median" radii of the three extinction coefficient distributions can also be estimated; hence, droplets smaller than or equal to these "median" radii would make up 50 percent contribution to spectral attenuation, or doubling the contribution in this range would give the total extinction coefficient of the normalized drop-size distribution. Table 2 shows these radii and the liquid water contained in sizes up to the "median" radius, the percentage contribution of the haze regime, and the total number density or concentration which were extracted from the processed data. The haze regime which contains negligible amount of liquid water is that portion of a fog whose distribution appears to be separate from that of the fog regime and whose particles are submicron in size, generally no greater than 1μm to 2μm in radius.[10,4] The drop-size data indicated that the haze regime lay below about 1.25μm radius, but 1μm radius was used as the dividing line in the analysis.

These figures are not restricted to the study of the spectral median radius alone. The percentage contributions to spectral attenuation in any size intervals can be readily obtained. Next, the Meppen fog will be examined in detail and the Fort Ord fogs will be mentioned only to illuminate certain observations.

Table 2 shows that the fog evolution is well reflected in the size changes as a function of time of the statistical median radius. Corresponding changes of the median radii are also found in the 0.55μm and 3.80μm spectral regions. Note the changes with time of the size differences between

[10]E. E. Hindman II, and O. E. R. Heimdahl, 1977, "Submicron Haze Droplets and Their Influence on Visibility in Fog," Preprints: 6th Conference on Inadvertent and Planned Weather Modification, American Meteorological Society, Boston, 10-13

[4]Richard D. H. Low, Louis D. Duncan, and Y. Y. Roger R. Hsiao, 1979, "Microphysical and Optical Properties of California Coastal Fogs at Fort Ord," ASL-TR-0034, US Army Atmospheric Sciences Laboratory, ERADCOM, White Sands Missile Range, NM

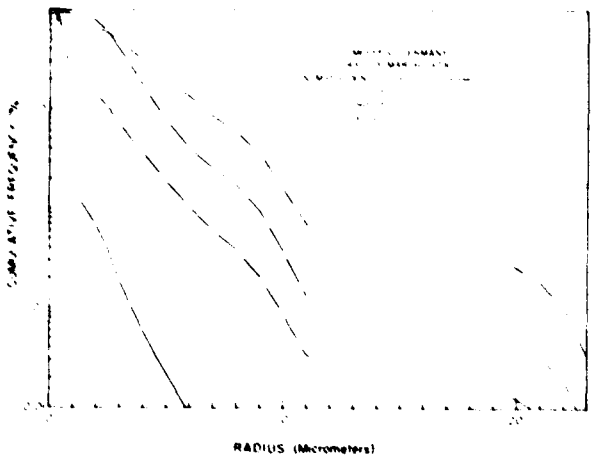

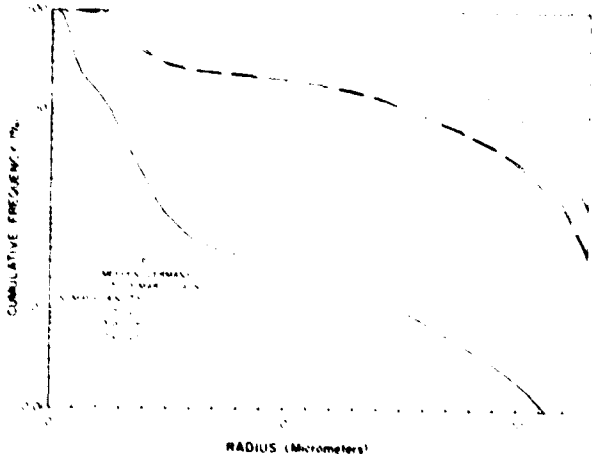

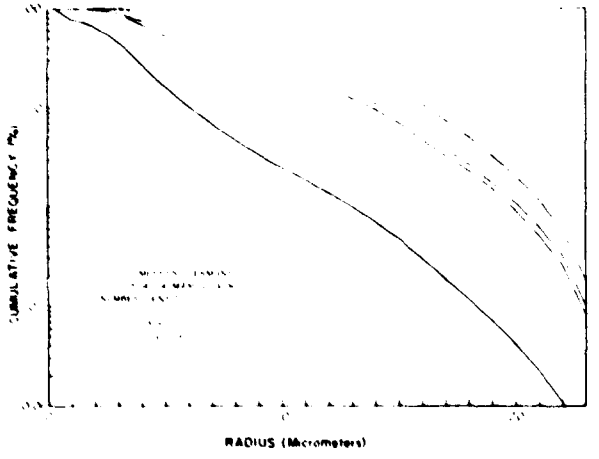

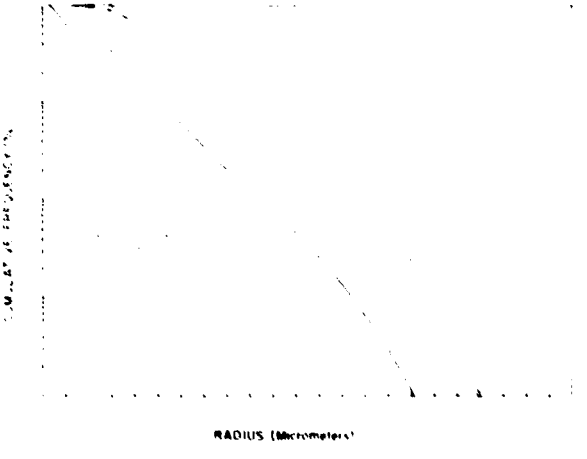

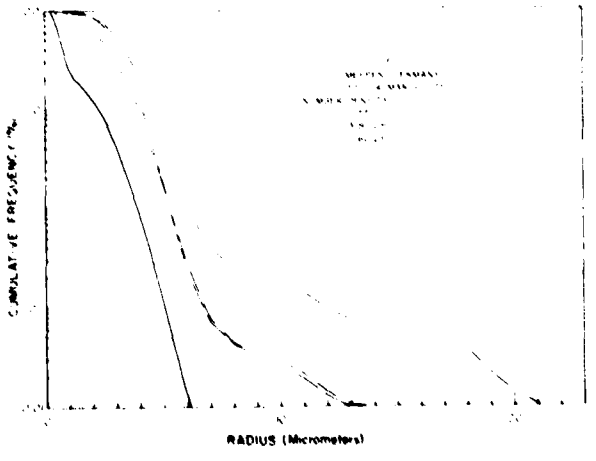

Figure 7 (a through e). Percentage cumulative frequencies in number density and in three spectral regions as a function of time, Meppen, Germany, 3-4 March 1978.

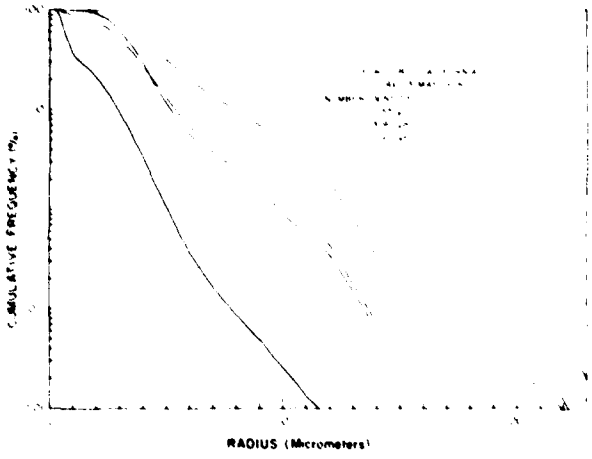

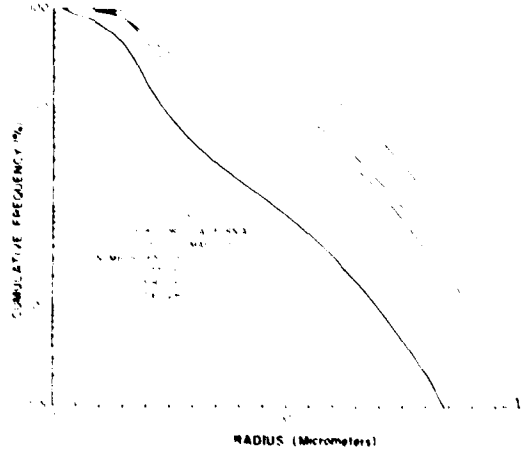

Figure 8 (a and b). Percentage cumulative frequencies in number density and in three spectral regions as a function of time, Fort Ord, California, 3 May 1978.

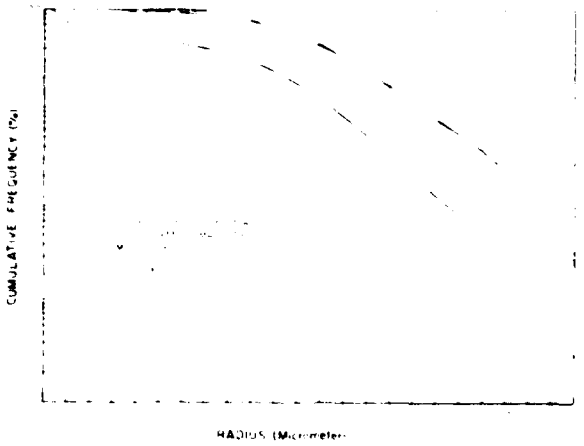

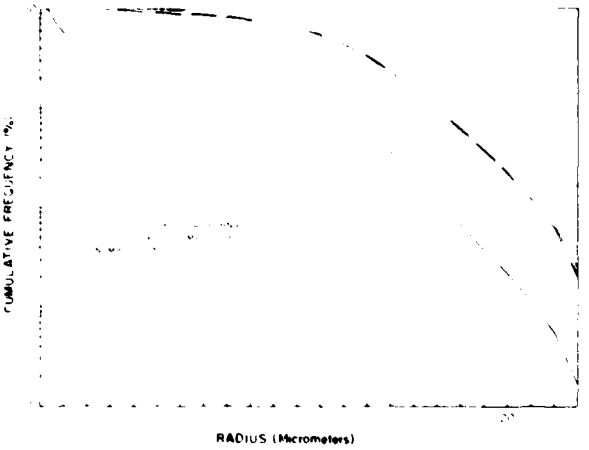

Figure 9 (a and b). Percentage cumulative frequencies in number density and in three spectral regions as a function of time, Fort Ord, California, 9 May 1978.

TABLE 2. FIFTY PERCENT CONTRIBUTION TO SPECTRAL ATTENUATION BY DROPLETS SMALLER THAN OR EQUAL TO THE "MEDIAN" RADIUS AT EACH WAVELENGTH AND THE PERCENTAGE AMOUNT OF LIQUID WATER CONTENT (LWC) CONTAINED THEREIN. ALSO SHOWN IS THE FRACTIONAL CONTRIBUTION OF THE HAZE REGIME BELOW 1 μm RADIUS

Time	Median		0.55 μm		[illegible] μm		[illegible] μm		[illegible]
	r (μm)	LWC (%)	r (μm)	LWC (%)	r (μm)	LWC (%)	r (μm)	LWC (%)	
	Haze (%)		Haze (%)		Haze (%)		Haze (%)		
	Meppen, Germany, 3-4 March 19[illegible]								
1832	0.40	0.7	0.50	17.6	2.60	[illegible]	[illegible]	[illegible]	[illegible]
	98.0		80.6		[illegible]		[illegible]		
2217	0.75	0.8	3.10	15.2	[illegible]	[illegible]	[illegible]	[illegible]	[illegible]
	68.4		15.3		[illegible]		[illegible]		
0114	2.70	2.3	6.30	26.4	[illegible]	[illegible]	[illegible]	[illegible]	[illegible]
	21.3		0.7		[illegible]		[illegible]		
0539	1.70	0.8	[illegible]	[illegible]	[illegible]	[illegible]	[illegible]	[illegible]	[illegible]
	37.1		2.2		[illegible]		[illegible]		
1000	0.73	1.9	2.50	27.6	[illegible]	[illegible]	[illegible]	[illegible]	[illegible]
	73.3		[illegible]		[illegible]		[illegible]		
	Fort Ord, California, [illegible] May 19[illegible]								
[illegible]	0.75	[illegible]	[illegible]	28.4	[illegible]	[illegible]	[illegible]	[illegible]	[illegible]
	64.3		[illegible]		[illegible]		[illegible]		
[illegible]	2.80	6.5	[illegible]	29.3	[illegible]	[illegible]	[illegible]	[illegible]	[illegible]
	14.6		[illegible]		[illegible]		[illegible]		
	Fort Ord, California, [illegible] May 19[illegible]								
[illegible]	[illegible]	[illegible]	12.20	36.6	12.20	36.6	[illegible]	[illegible]	[illegible]
	[illegible]		0.5		[illegible]		[illegible]		
[illegible]	4.70	[illegible]	11.40	35.7	11.40	35.7	[illegible]	[illegible]	[illegible]
	97.8		0.3		[illegible]		[illegible]		

the median radii in these two spectral regions. From 2217 hours on, the median radii in the 3.80μm region became comparable with those in the 0.55μm region. As mentioned previously, at about 2217 hours in figure 1 (a and b) the extinction coefficient in the 3.80μm region crossed over the 0.55μm coefficient and then remained above the latter for good. The same change was also observed in the Fort Ord fogs. In contrast, the same cannot be said of the percentages of liquid water content in these fogs. Yet, in the 10.6μm region, the median radius departed little from the statistical median-volume radius which, by definition, is the radius of the droplet such that half the water is contained in larger (or smaller) droplets.

As regards the haze regime, which was discussed in the preceding section, the changes with time of its magnitudes correspond very well in both the statistical and the optical domains. Its predominant effect on visible transmission during the fog formation stage and, to a lesser extent, during the dissipation stage is well displayed in table 2. However, its effect on 3.80μm transmission diminished appreciably and became almost negligible in the 10.6μm region. Only when the fog became fully grown and attained maturity did the effect of the haze regime nearly disappear from 0114 to about 0539 hours. An explanation for the interaction between haze and fog particles was offered by Low.[4]

3.4 Regression Relationship between Spectral Attenuation and Liquid Water Content

One of the technical goals of the DOD plan for atmospheric transmission research and development, mentioned at the beginning of this report, is to accurately model the propagation effects of naturally occurring aerosols. Models may be empirical or physical. The former are usually derived from experimental data and the latter from the so-called first principles such that haze and fog formation, transport, and dissipation may be modeled in relation to measurable or predictable meteorological parameters. The haze and fog data collected by this laboratory in the past as well as data reported in the literature do not lend themselves to development of physical models. The meteorological descriptions of fog and/or haze were, without exception, sketchy or, oftentimes, none at all. There is no way to develop physical models on the basis of such data. Until haze and fog data become available (collected specifically with the development of physical models in mind), the approach at present must therefore be empirical.

[4]Richard D. H. Low, Louis D. Duncan, and Y. Y. Roger R. Hsiao, 1979, "Microphysical and Optical Properties of California Coastal Fogs at Fort Ord," ASL-TR-0034, US Army Atmospheric Sciences Laboratory, ERADCOM, White Sands Missile Range, NM

The liquid water content of a fog will be used as the common parameter to be related to spectral attenuation at three wavelengths. It is a convenient parameter to use since extinction coefficients at any wavelengths which correlate well with liquid water content will be mutually correlated. The Meppen and the Fort Ord fog drop-size data were processed to produce liquid water contents and extinction coefficients in the 0.55μm, 3.80μm, and 10.6μm spectral regions. These derived data were then plotted on full-log papers separately and collectively so as to generate different regression equations and thus enable regression analysis to be performed. In this section the regression equations will be dealt with first, and then a brief regression analysis will be performed to find out if these equations, and hence these fogs, are similar or different statistically.

3.5 Regression Equations

When the liquid water and spectral extinction data were plotted in scatter diagrams on full-log papers, a linear relationship in log space appeared to exist between them (as demonstrated in the visible region by several other authors[1,12,13,14]). The form of the regression lines on the basis of a least-square fit can be represented by

$$\beta = a\, W^{b} , \qquad (4)$$

where β, a function of wavelength, is the extinction coefficient; a and b are the regression coefficients, also functions of wavelength; and W is the liquid water content. Figures 10 to 12 present the scatter diagrams together with the regression lines and the so-called prediction bands. Figures 10 and 11 show that three separate regression lines be derived from each set of the fog data. To keep these figures uncluttered, only the overall lines are displayed.

---

[1]H. G. Houghton, and W. H. Radford, 1938, "On the Measurement of Drop-Size and Liquid Water Content in Fogs and Clouds," Papers in Physical Oceanography and Meteorology, Vol VI, No 4

[12]R. G. Eldridge, 1966, "Haze and Fog Aerosol Distributions," J Atmospheric Sci, 23:605-613

[13]M. Kumai, 1973, "Arctic Fog Droplet Size Distribution and Its Effect on Light Attenuation," J Atmospheric Sci, 30:635-643

[14]R. G. Pinnick, D. L. Hoihjelle, G. Fernandez, E. B. Stenmark, J. D. Lindberg, G. B. Hoidale, and S. G. Jennings, 1978, "Vertical Structure in Atmospheric Fog and Haze and Its Effects on Visible and Infrared Extinction," J Atmospheric Sci, 35:2020-2032

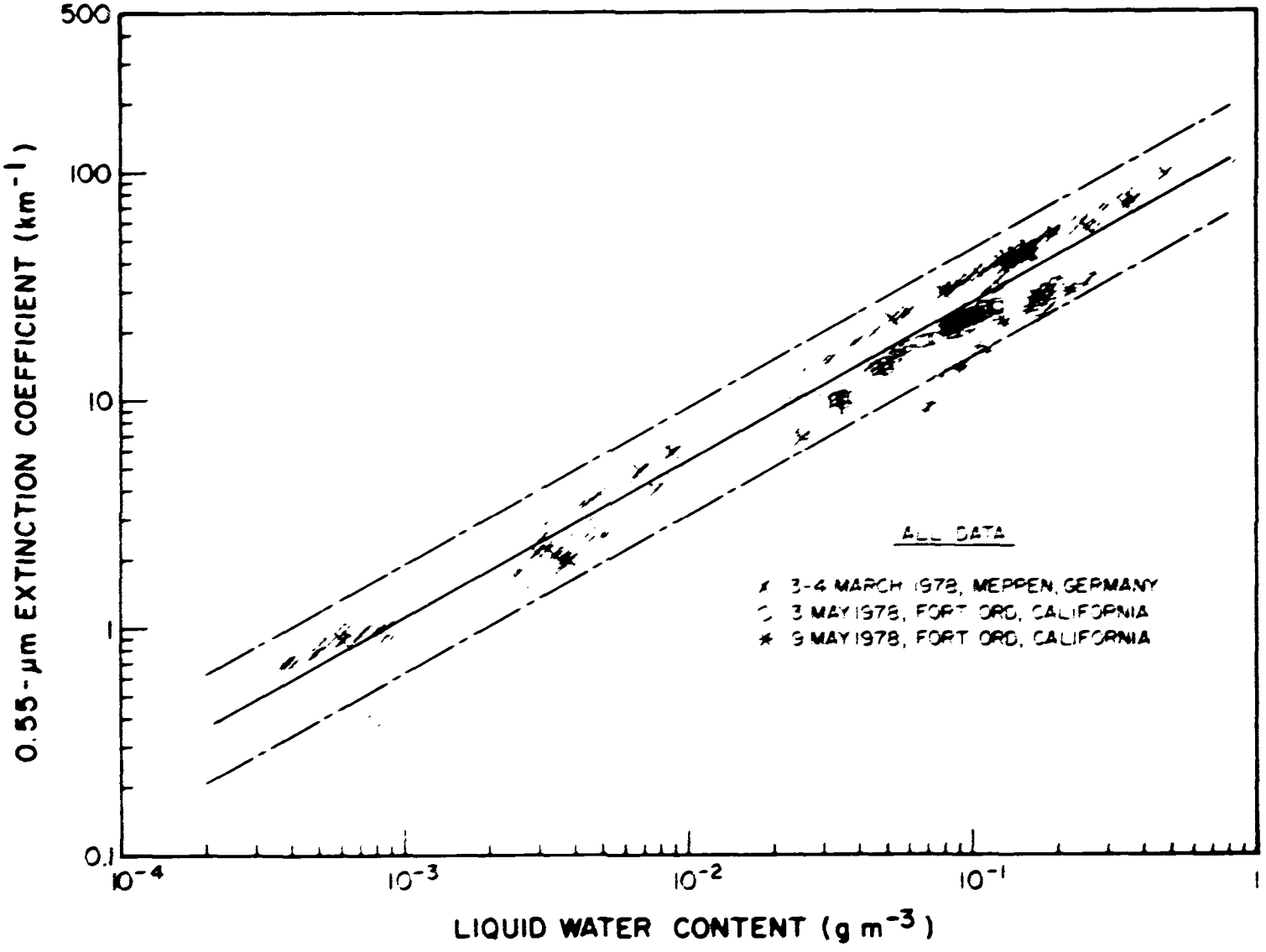

Figure 10. The regression line derived from all fog data relating 0.55-μm extinction coefficient to liquid water content bounded by the 95 percent prediction band.

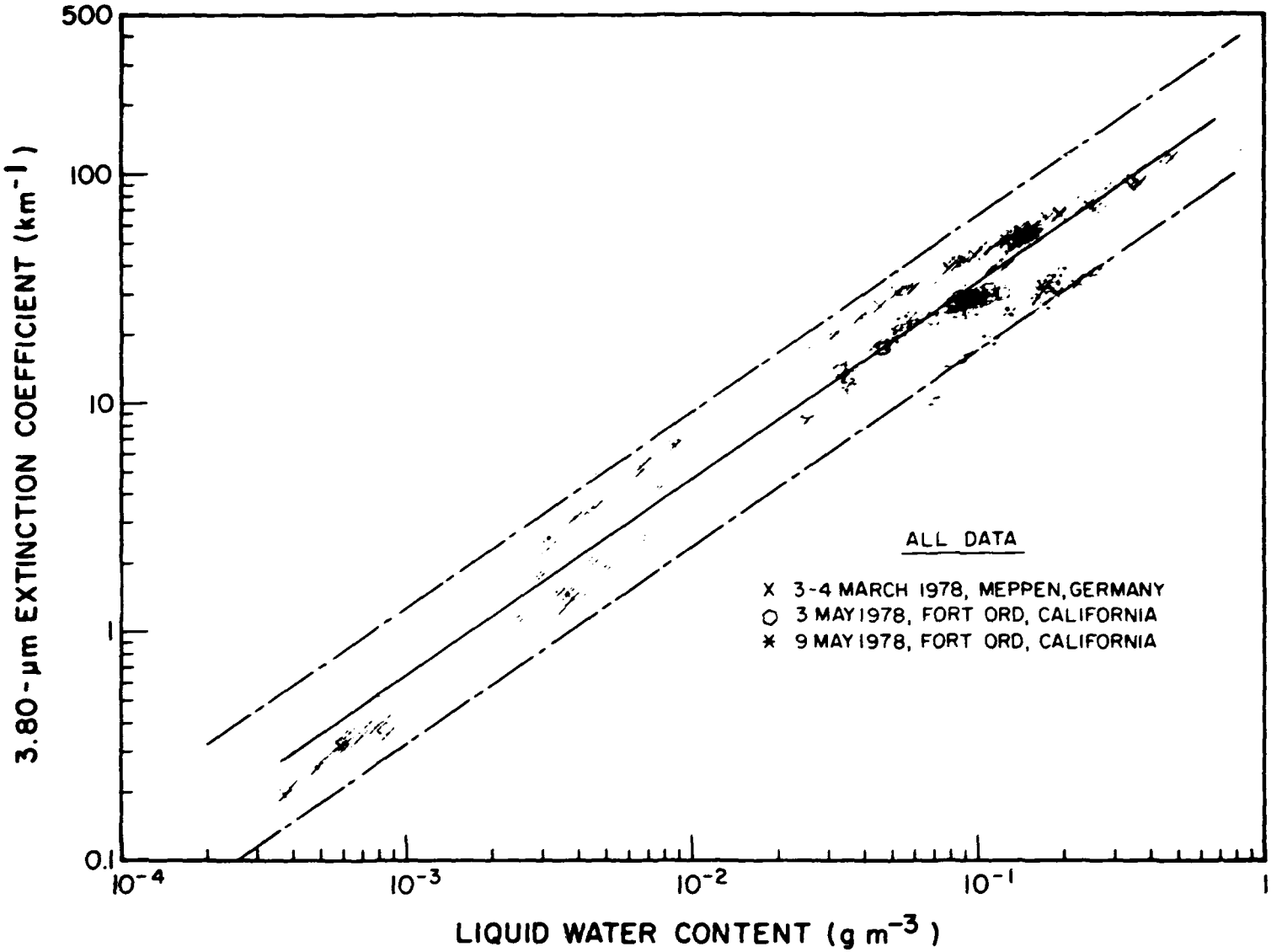

Figure 11. The regression line derived from all fog data relating 3.80 μm extinction coefficient to liquid water content bounded by the 95 percent prediction band.

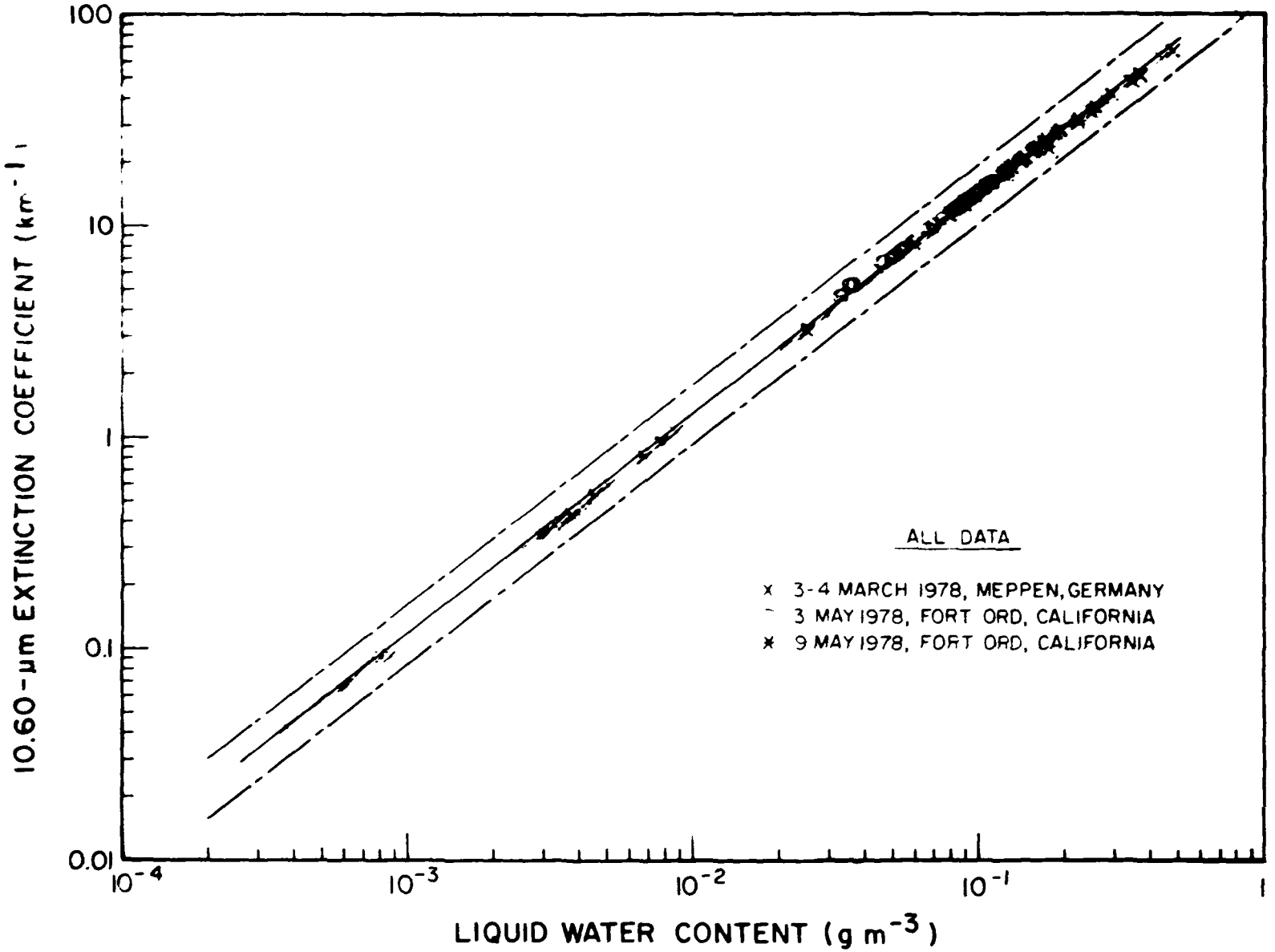

Figure 12. The regression line derived from all fog data relating 10.6-m extinction coefficient to liquid water content bounded by the 95 percent prediction band.

The regression coefficients in different spectral regions for individual as well as collective fog cases are listed in table 3. In figure 10, there appeared to be a group of data in the Meppen fog in which perfect linear correlation in log space existed between 0.55μm extinction and liquid water content. All other data points fell below this perfect regression line; that is, in the data range considered, for the same amount of liquid water, these points would give lower extinction values. In figure 11, which relates 3.80μm extinction to liquid water, the same group of data no longer represented a straight-line fit but more like a quadratic fit on log paper. All other data points would again give lower extinction values for the same liquid water content. In figure 12, which concerns the 10.6μm region, the straight-line fit is nearly perfect for all three fogs. That is why in table 3 only one set of regression coefficients is given although some insignificant differences in coefficients did exist when each fog was fitted separately. A discussion of these observations and their implications will be presented in the following section.

3.6 Regression Analysis

It is already known that these three fog episodes belonged in different fog types. Not only that, two fogs came from one place, and one fog from another. One would instinctively surmise that one model cannot cover them all. Nevertheless, it would be of academic, if not practical, interest to ascertain statistically whether the fogs were different and whether a single model might suffice. To be able to carry out a simple linear regression analysis, equation (4) is transformed into the following linear expression:

$$Y = A + B X , \tag{5}$$

where $Y = \log_{10}\beta$, $A = \log_{10}a$, and $X = \log_{10}W$. In the course of deriving a least-squares fit, the statistics necessary for regression analysis are not difficult to calculate. These statistics are listed in tables 4 and 5 for the 0.55μm and 3.80μm spectral regions, respectively; namely, number density, N; mean X, $\overline{X}$; mean Y, $\overline{Y}$; variance of Y, V(Y); sum of X squares, $S(X^2)$; and correlation coefficient, R.

A cursory examination of the two tables shows that by themselves, with the possible exception of the last case in table 5, linear regression is acceptable if considering the correlation coefficients alone. A table was not prepared for the 10.6μm region since the table would be superfluous. The correlation coefficient for the line in figure 12 is 0.994, and the value from the F-test or the ratio of mean squares due to regression to that due to residual is 3.34×10^5. For a perfect regression line, the ratio, of course, would be infinity; that is, no part of the line cannot be explained.

TABLE 3. REGRESSION COEFFICIENTS IN THE 0.55μm, 3.80μm, AND 10.6μm SPECTRAL REGIONS FOR ALL AS WELL AS INDIVIDUAL FOG CASES

Fog Cases	0.55μm		3.80μm		10.6μm	
	a	b	a	b	a	b
All	130.81	0.692	242.82	0.859	155.22	1.042
Meppen	162.00	0.721	315.04	0.901	155.22	1.042
Fort Ord (3 May 72)	171.09	0.845	213.05	0.836	155.22	1.042
Fort Ord (9 May 72)	147.10	0.986	165.61	0.984	155.22	1.042
Fort Ord (All)	113.00	0.735	124.83	0.693	155.22	1.042

TABLE 4. STATISTICAL PARAMETERS REQUIRED FOR COMPARING REGRESSION LINES IN THE 0.55μm SPECTRAL REGION

Fog Cases	N	$\overline{X}$	$\overline{Y}$	A	B	V(Y)	$S(X^2)$	R
All	241	-1.475	1.095	2.117	0.692	0.01445	156.78	0.98
Meppen	170	-1.633	1.032	2.210	0.721	0.00937	133.31	0.99
Fort Ord (3 May 78)	48	-1.221	1.201	2.233	0.845	0.00121	6.136	0.98
Fort Ord (9 May 78)	23	-0.838	1.341	2.168	0.986	0.00209	0.664	0.97
Fort Ord (All)	71	-1.097	1.246	2.053	0.735	0.00762	9.084	0.95

TABLE 5. STATISTICAL PARAMETERS REQUIRED FOR COMPARING REGRESSION LINES IN THE 3.80μm SPECTRAL REGION

Fog Cases	N	$\overline{X}$	$\overline{Y}$	A	B	V(Y)	$S(X^2)$	R
All	241	-1.475	1.118	2.385	0.859	0.0224	156.78	0.96
Meppen	170	-1.633	1.027	2.498	0.901	0.0170	133.31	0.97
Fort Ord (3 May 78)	48	-1.221	1.308	2.328	0.836	0.0026	6.136	0.97
Fort Ord (9 May 78)	23	-0.838	1.394	2.219	0.984	0.0026	0.664	0.92
Fort Ord (All)	71	-1.097	1.336	2.096	0.693	0.0124	9.084	0.84

The correlation for each case in table 5 for the 3.80μm region is not as good as that in table 4 when both the residual mean squares and the correlation coefficients are considered. Therefore, an analysis of table 4 would suffice; any inferences drawn here would be applicable to those cases in table 5. The intercepts and slopes of each pair will be compared. Since the sample size is sufficiently large, the normal Z test can be used instead of the student t test. At the 5 percent significance level, the Z-value is 1.96, and table 6 was prepared. Only the Fort Ord fogs shared the overall model or scaling law of the three fogs. No two fogs are alike statistically although the Meppen fog and the two Fort Ord fogs seem to share the same intercept. On the other hand, depending on sensor system specifications and laboratory requirements, the overall models presented in figures 10 to 12 may well serve the purpose. To this end, the prediction interval or band was drawn in each figure at the 5 percent significance level; that is, given a liquid water content value, the extinction coefficient will lie within this band 95 percent of the time.

4. DISCUSSION

In this section an attempt will be made to relate the derived models to fog optical and microphysical properties, and the latter's implications in the formulation of these models in the three spectral regions will be discussed.

4.1 The 0.55μm Spectral Region

As already mentioned, quite a substantial number of data points in the Meppen fog appeared to give a nearly perfect linear relationship between visible extinction and liquid water content. To find out what made this set of data so well-behaved, a freehand straight line was drawn through these points, which yielded the following regression equation:

$$\beta = 175.79\ W^{0.704}\ , \qquad (6)$$

whose slope does not differ significantly from that of the overall regression equation. To determine which data points would satisfy this equation, the liquid water content was allowed to vary by ±14 percent, thereby generating extinction coefficients which vary about ±10 percent. Then all the 170 Meppen data points were run through this ±10 percent interval and those lying in this interval were picked out and compared with the original data while the times of their occurrences were noted. The results were that while some points were contained during the fog's formation stage the rest of them were found in the period from about 0240 through about 0930 hours with a few out of place here and there.

TABLE 6. Z-TEST AT 5% SIGNIFICANCE LEVEL OF THE SLOPES AND INTERCEPTS OF TWO REGRESSION LINES

Fog Cases	Z-Test	All	Meppen	Fort Ord (3 May 78)	Fort Ord (9 May 78)	Fort Ord (All)
All	Slope	0	2.28	8.99	5.17	1.41
	Intercept	0	4.15	4.82	1.01	1.72
Meppen	Slope	2.28	0	7.58	4.67	0.46
	Intercept	4.15	0	0.97	0.83	4.26
Fort Ord (3 May 78)	Slope	8.99	7.58	0	2.44	3.42
	Intercept	4.82	0.97	0	1.27	4.75
Fort Ord (9 May 78	Slope	5.17	4.67	2.44	0	3.98
	Intercept	1.01	0.83	1.26	0	1.97
Fort Ord (All)	Slope	1.41	0.46	3.42	3.98	0
	Intercept	1.72	4.26	4.75	1.97	0

It is in this period designated as the mature or stable phase of the Meppen fog (figure 1b) that the three extinction coefficients appeared to march in orderly steps. During the other periods, the data points all lay below this line. In fact, one or more regression equations could be derived from this set of data which one would expect to be different from either equation (6) or the overall equation. The mature stage was marked by a moderate haze regime (figure 4d and table 2), maximum mode radius in the fog sector (table 1), minimum ratio in number density of the first mode to the second (table 2), near maximum spectral "median" radius (table 2).

In the case of the 3 May advection fog, all data points appeared to lie quite close to the overall regression line and seemed to be well-behaved, conceivably an indication of maturity and stability. By comparison, all the data points of the 9 May radiation-advection fog were below the overall line and appeared to form a lower boundary to the overall line. The points by themselves, however, seemed to be fairly well organized.

Depending on the requirements, the three fogs may call for three different representations. Moreover, the Meppen fog by itself may be modeled by two regression lines, each depicting a different stage of its life history. On the other hand, if the requirements are not too stringent, a single model or scaling law for all three fogs might suffice.

4.2 The 3.80μm Spectral Region

The preceding discussion on the 0.55μm spectral region is equally applicable to this region, except that the straight-line sector of the Meppen fog now became parabolic. However, this is not too discernible in the Fort Ord fogs, perhaps because of the paucity of data. Nevertheless, note that in Pinnick et al[14] the same parabolic trend may be detected in their figure 10c. Perhaps a quadratic fit should be considered.

4.3 The 10.6μm Spectral Region

Since the linear relationship between extinction and liquid water content is so nearly perfect in the 10.6μm region despite the diversity of fogs in origin and type, this relationship could be taken advantage of. The relationship strongly indicates that the liquid water content of a fog can be derived from transmission measurement in the 10.6μm region. Following measurements of transmittances in a fog chamber at different wavelengths,

[14] R. G. Pinnick, D. L. Hoihjelle, G. Fernandez, E. B. Stenmark, J. D. Lindberg, G. B. Hoidale, and S. G. Jennings, 1978, "Vertical Structure in Atmospheric Fog and Haze and Its Effects on Visible and Infrared Extinction," J Atmospheric Sci, 35:2020-2032

Carlon et al[15] suggested precisely that kind of measurement in the 10.5μm region. In a quasi-theoretical approach, Chylek[16] showed that the liquid water content of a fog or cloud can be readily found regardless of its drop-size distributions by means of transmission measurements at the 11.0μm wavelength if the largest droplet in the fog or cloud is no larger than 14μm radius. The fog chamber which Carlon et al[15] used in their experiments produced droplets probably no larger than 10μm radius. Therefore, both sides came to the same conclusion.

The fogs used for this report had sizes far beyond 10μm in radius most of the time, yet there existed a nearly perfect correlation between 10.6μm extinction and liquid water content. The same may be found in Pinnick et al[14] in their figure 10d, although they used the 10.0μm wavelength. Thus, it seems that a 10.6μm CO_2 laser may be used in a device designed so that the liquid water content in a finite volume over a path length may be obtained.

5. CONCLUSIONS

The Meppen fog which occurred on 3 to 4 March 1978 was analyzed in detail both spectrally and microphysically. Spectral evolution was examined in relation to drop-size evolution in an attempt to gain some insight in the complex nature of establishing optical models or scaling laws and hence to better judge the adequacy of a model or a law.

The magnitude of the haze regime of a fog, often a reflection of the pollution level at a locality, showed a strong influence on the microphysical properties and hence the optical characteristics of the haze regime. Generally, the dominance of the haze regime in the early life of a fog, which severely affects the transmission in the 0.55μm and 3.80μm regions, hinders a working relationship between extinction and liquid water due to its tiny particle sizes and water deficiency. As the fog grows into maturity laden

[15]H. R. Carlon, D. H. Anderson, M. E. Milham, T. L. Tamove, R. H. Frickel, and I. Sindoni, 1977, "Infrared Extinction Spectra of Some Common Liquid Aerosols," Appl Opt, 16:1598-1605

[16]P. Chylek, 1978, "Extinction and Liquid Water Content of Fogs," J Atmospheric Sci, 35:296-300

[14]R. G. Pinnick, D. L. Hoihjelle, G. Fernandez, E. B. Stenmark, J. D. Lindberg, G. B. Hoidale, and S. G. Jennings, 1978, "Vertical Structure in Atmospheric Fog and Haze and Its Effects on Visible and Infrared Extinction," J Atmospheric Sci, 35:2020-2032

with plenty of water and as its haze regime decreases in size and influence, this relationship becomes more tractable in these two spectral regions. As the fog becomes aged and approaches dissipation, although its haze regime may have regained some strength, the fog sector is still quite water laden despite the depletion of its larger droplets, and the relationship between extinction and liquid water is still relatively tractable. From this study of the Meppen fog, indications are strong that a linear relationship exists in the visible region, except perhaps at extremely low liquid water content of the order of 10^{-4} g m^{-3} or less, and in the 3.80μm region there may be a quadratic relationship. By contrast, in the 10.6μm region the relationship is almost perfectly linear, thus the suggestion that liquid water content be obtained by means of transmittance measurements using a 10.6μm CO_2 laser.

As was noted in a preceding section, the Meppen fog may be represented by a comprehensive regression line, a line according to equation (6), or one or more lines derived without those data points used to generate equation (6). However, the comprehensive line encompassed the complete drop-size data set; its completeness lies in the fact that it represents the Meppen fog's entire life history. Consequently, not much attention was given to the Ford Ord fogs in this analysis. It is imperative that an optical model representing a fog be built on the foundation of a complete set of data, spanning fog formation through dissipation rather than a set depicting an unknown phase of its life cycle, unless it can be demonstrated statistically that the model derived from the former does not differ significantly from the latter. Only in this way may the relative validity of the models allegedly representing different haze and fog types be assessed.

Five models or scaling laws in each of the three spectral regions are presented: one each for the three fogs, one for all, and one for the California coastal fogs. Statistically and genetically, these fogs are different. By itself, the least-squares fit for each case in the visible is quite respectable if its correlation coefficient means anything. In fact, when all the fog data are taken together, the fit is no less respectable, neglecting the fact that only certain phases of the Ford Ord fogs were portrayed, and the prediction bands at the 5 percent significance level appear to justify this observation.

Finally, it should be emphasized that with the possible exception of the Meppen model which represents one type of fog occurring in the Meppen area, the Fort Ord models must be used with caution for reasons already discussed. Again, whether one model or scaling law would suffice or more than one is needed depends entirely upon the sensitivities and requirements of the electro-optical sensors to be deployed. When a heavy fog became fully grown, sensors operating in wavelength regions other than the 10.6μm were so degraded that they were rendered ineffective. However, those in the 10.6μm region could operate most of the time. Then, modeling the heavy fogs may become a moot question.

REFERENCES

1. Houghton, H. G., and W. H. Radford, 1938, "On the Measurement of Drop-Size and Liquid Water Content in Fogs and Clouds," Papers in Physical Oceanography and Meteorology, Vol VI, No 4.

2. Stewart, D. A., 1977, "Infrared and Submillimeter Extinction by Fog," Technical Report TR-77-9, Technology Laboratory, Physical Science Directorate, Redstone Arsenal, AL.

3. Low, Richard D. H., Louis D. Duncan, and Richard B. Gomez, 1978, "The Microphysical Basis of Fog Optical Characterization," ASL-TR-0011, US Army Atmospheric Sciences Laboratory, ERADCOM, White Sands Missile Range, NM.

4. Low, Richard D. H., Louis D. Duncan, and Y. Y. Roger R. Hsiao, 1979, "Microphysical and Optical Properties of California Coastal Fogs at Fort Ord," ASL-TR-0034, US Army Atmospheric Sciences Laboratory, ERADCOM, White Sands Missile Range, NM.

5. Lindberg, J. D., 1979, Private communications.

6. Low, Richard D. H., 1975, "Microphysical Evolution of Fog," J Research Atmosphere, 2:23-32.

7. Pilié, R. J., E. J. Mack, W. C. Kocmond, W. J. Eadie, and C. W. Rogers, 1975, "The Life Cycle of Valley Fogs: Part II: Fog Microphysics," J Appl Meteorol, 14:364-374.

8. Roach, W. T., R. Brown, S. J. Caughly, J. A. Garland, and C. J. Readings, 1976, "The Physics of Radiation Fogs: Ia-Field Study," Quart J Roy Meteorol Soc, 102:313-333.

9. Goodman, J., 1977, "The Microstructure of California Coastal Fog and Stratus," J Appl Meteorol, 16:1056-1067.

10. Hindman II, E. E., and O. E. R. Heimdahl, 1977, "Submicron Haze Droplets and Their Influence on Visibility in Fog," Preprints: 6th Conference on Inadvertent and Planned Weather Modification, American Meteorological Society, Boston, 10-13.

11. Rodhe, B., 1962, "The Effect of Turbulence on Fog Formation," Tellus, 14:49-86.

12. Eldridge, R. G., 1966, "Haze and Fog Aerosol Distributions," J Atmospheric Sci, 23:605-613.

13. Kumai, M., 1973, "Arctic Fog Droplet Size Distribution and Its Effect on Light Attenuation," J Atmospheric Sci, 30:635-643.

14. Pinnick, R. G., D. L. Hoihjelle, G. Fernandez, E. B. Stenmark, J. D. Lindberg, G. B. Hoidale, and S. G. Jennings, 1978, "Vertical Structure in Atmospheric Fog and Haze and Its Effects on Visible and Infrared Extinction," J Atmospheric Sci, 35:2020-2032.

15. Carlon, H. R., D. H. Anderson, M. E. Milham, T. L. Tamove, R. H. Frickel, and I. Sindoni, 1977, "Infrared Extinction Spectra of Some Common Liquid Aerosols," Appl Opt, 16:1598-1605.

16. Chýlek, P., 1978, "Extinction and Liquid Water Content of Fogs," J Atmospheric Sci, 35:296-300.

17. Pinnick, R. G. and H. J. Auvermann, 1979, "Response Characteristics of Knollenberg Light-Scattering Aerosol Counters," J Aerosol Sci, 10:55-74.

ELECTRO-OPTICS DIVISION DISTRIBUTION LIST

Commander
US Army Aviation Center
ATTN: ATZQ-D-MA
Fort Rucker, AL 36362

Commander
US Army Aviation School
Fort Rucker, AL 36362

Ballistic Missile Defense Advanced Technology Center
ATTN: ATC-R
PO Box 1500
Huntsville, AL 35807

Lockheed-Huntsville Msl & Space Co.
ATTN: Dr. Lary W. Pinkley
PO Box 1103
West Station
Huntsville, AL 35807

Chief, Atmospheric Sciences Div
Code ES-81, NASA
Marshall Space Flight Center,
AL 35812

Project Manager
Patriot Missile Systems
ATTN: DRCPM-MD-T
Redstone Arsenal, AL 35809

Commander
US Army Missile R&D Command
ATTN: DRDMI-CGA (B. W. Fowler)
Redstone Arsenal, AL 35809

Redstone Scientific Information Center
ATTN: DRDMI-TBD
US Army Missile R&D Command
Redstone Arsenal, AL 35809

Commander
US Army Missile R&D Command
ATTN: DRDMI-TEM (R. Haraway)
Redstone Arsenal, AL 35809

Commander
US Army Missile R&D Command
ATTN: DRDMI-TRA (Dr. Essenwanger)
Redstone Arsenal, AL 35809

Commander
US Army Missiles and Munitions Center & School
ATTN: ATSIC-CD
Redstone Arsenal, AL 35809

Commander
US Army Missile R&D Command
ATTN: DRDMI-REO (Dr. Maxwell Harper)
Redstone Arsenal, AL 35809

Commander
US Army Missile R&D Command
ATTN: DRDMI-RRE (Dr. Julius Lilly)
Redstone Arsenal, AL 35809

Commander
US Army Missile R&D Command
ATTN: DRDMI-TEO (Dr. Gene Widenhofer)
Redstone Arsenal, AL 35809

Commander
US Army Missile R&D Command
ATTN: DRDMI-HRO (Dr. D.B. Guenter)
Redstone Arsenal, AL 35809

Commander
US Army Missile R&D Command
ATTN: DRDMI-TDO (Dr. Hugh Anderson)
Redstone Arsenal, AL 35809

Commander
US Army Missile R&D Command
ATTN: DRDMI-YLA (Mr. W.S. Rich)
Redstone Arsenal, AL 35809

Commander
US Army Missile R&D Command
ATTN: DRDMI-TEG (Dr. George Emmons)
Redstone Arsenal, AL 35809

Commander
HQ, Fort Huachuca
ATTN: Tech Ref Div
Fort Huachuca, AZ 85613

Commander
US Army Intelligence Center & School
ATTN: ATSI-CD
Fort Huachuca, AZ 85613

Commander
US Army Intelligence Center & School
ATTN: ATSI-CD-CS (Mr. Jim Rustenbeck)
Fort Huachuca, AZ 85613

Commander
US Army Intelligence Center & School
ATTN: ATSI-CD-MD
Fort Huachuca, AZ 85613

Commander
US Army Communications Command
Fort Huachuca, AZ 85613

Commander
US Army Yuma Proving Ground
ATTN: Technical Library
Bldg 2100
Yuma, AZ 85364

Northrop Corporation
Electro-Mechanical Division
ATTN: Dr. R. D. Tooley
500 East Orangethorpe Ave
Anaheim, CA 92801

Naval Weapons Center
ATTN: Code 3173 (Dr. A. Shlanta)
China Lake, CA 93555

Hughes Helicopters
ATTN: Charles R. Hill
Centinela and Teale Streets
Culter City, CA 90230

Commander
US Army Combat Dev Evaluation Command
ATTN: ATEC-PL-M (Gary Love)
Fort Ord, CA 93941

SRI International
ATTN: Dr. Ed Uthe
333 Ravenswood Avenue
Menlo Park, CA 94025

SRI International
ATTN: J. E. Van der Laan
333 Ravenswood Avenue
Menlo Park, CA 94025

Sylvania Elec Sys Western Div
ATTN: Technical Reports Library
PO Box 205
Mountain View, CA 94040

Geophysics Officer
PMTC Code 3250
Pacific Missile Test Center
Point Mugu, CA 93042

Commander
Naval Ocean Systems Center
ATTN: Code 4473 (Tech Library)
San Diego, CA 92152

Commander
Naval Ocean Systems Center
ATTN: Code 532 (Dr. Juergen Richter)
San Diego, CA 92152

General Electric -TEMPO
ATTN: Dr. James Thompson
816 State Street
PO Drawer QQ
Santa Barbara, CA 93102

The RAND Corporation
ATTN: Ralph Huschke
1700 Main Street
Santa Monica, CA 90406

National Center for Atmos Research
NCAR Library
PO Box 3000
Boulder, CO 80307

Library-R-51-Tech Reports
NOAA/ERL
320 S. Broadway
Boulder, CO 80302

Wave Propagation Laboratory
NOAA/ERL
ATTN: Dr. Vernon Derr
Boulder, CO 80302

Particle Measuring Systems, Inc.
ATTN: Dr. Robert Knollenberg
1855 South 57th Court
Boulder, CO 80301

US Department of Commerce
Institute for Telecommunication Sciences
ATTN: Dr. H. J. Liebe
Boulder, CO 80303

HQDA (SAUS-OR/Hunter Woodall)
Rm 2E614, Pentagon
Washington, DC 20301

Dr. Herbert Fallin
ODUSA-OR
Rm 2E621, Pentagon
Washington, DC 20301

COL Elbert Friday
OUSDR&E
Rm 3D129, Pentagon
Washington, DC 20301

Defense Communications Agency
Technical Library Center
Code 205
Washington, DC 20305

Director
Defense Nuclear Agency
ATTN: Technical Library
Washington, DC 20305

Director
Defense Nuclear Agency
ATTN: RAAE (MAJ Ed Mueller)
Washington, DC 20305

Director
Defense Nuclear Agency
ATTN: SPAS (Mr. A.T. Hopkins)
Washington, DC 20305

Defense Intelligence Agency
ATTN: Scientific Advisory Committee
Washington, DC 20310

HQDA (DAMA-ARZ-D/Dr. Verderame)
Washington, DC 20310

HQDA (DAMI-ISP/Mr. Beck)
Washington, DC 20310

Department of the Army
Deputy Chief of Staff for
Operations and Plans
ATTN: DAMO-RQ
Washington, DC 20310

Department of the Army
Director of Telcommunications and
Command and Control
ATTN: DAMO-TCZ
Washington, DC 20310

Department of the Army
Deputy Chief of Staff for Research,
Development and Acquisition
ATTN: DAMA-AR
Washington, DC 20310

Department of the Army
Assistant Chief of Staff for Intelligence
ATTN: DAMI-TS
Washington, DC 20310

HQDA (DAEN-RDM/Dr. de Percin)
Forrestal Building
Washington, DC 20314

Director
Naval Research Laboratory
ATTN: Code 5530
Washington, DC 20375

Director
Naval Research Laboratory
ATTN: Code 2627
Washington, DC 20375

Director
Naval Research Laboratory
ATTN: Code 1409
(Dr. J. M. MacCallum)
Washington, DC 20375

Director
Naval Research Laboratory
ATTN: Code 5567
(Dr. James A. Dowling)
Washington, DC 20375

Director
Naval Research Laboratory
ATTN: Code 5567
(Dr. Steve Hanley)
Washington, DC 20375

Director
Naval Research Laboratory
ATTN: Code 8320
(Dr. L.H. Ruhnke)
Washington, DC 20375

The Library of Congress
ATTN: Exchange & Gift Div
Washington, DC 20540
2

Head, Atmos Rsch Section
Div Atmospheric Science
National Science Foundation
1800 G. Street, NW
Washington, DC 20550

ADTC/DLODL
Eglin AFB, FL 32542

Naval Training Equipment Center
ATTN: Technical Library
Orlando, FL 32813

Georgia Institute of Technology
ATTN: Dr. James Wiltse
Atlanta, GA 30332

Georgia Institute of Technology
ATTN: Dr. Robert McMillan
Atlanta, GA 30332

Georgia Institute of Technology
ATTN: Mr. James Gallagher
Atlanta, GA 30332

Commander
US Army Infantry Center
Fort Benning, GA 31805

Commander
US Army Infantry Center
ATTN: AT2B-CD
Fort Benning, GA 31805

US Army Signal School
ATTN: ATSN-CD
Fort Gordon, GA 30905

USAFETAC
Scott AFB, IL 62225

Commander
Air Weather Service
ATTN; DNPP (LTC Donald Hodges)
Scott AFB, IL 62269

Commander
US Army Combined Arms Center
ATTN: ATCA-CAA-Q (Kent Pickett)
Fort Leavenworth, KS 66027

Commander
US Army Combined Arms Center
ATTN: ATCA-CS
Fort Leavenworth, KS 66027

Commander
US Army Combined Arms Center
ATTN: ATCA-CCC
Fort Leavenworth, KS 66027

Commander
US Army Combined Arms Center
ATTN: ATCA-CDC
Fort Leavenworth, KS 66027

Commander
US Army Combined Arms Center
ATTN: ATCA-CDE
Fort Leavenworth, KS 66027

Commander
US Army Combined Arms Center
ATTN: ATCA-CCM
Fort Leavenworth, KS 66027

Commander
US Army Armor Center
ATTN: ATZK-AE-TA
(Dr. Charles Leake)
Fort Knox, KY 40121

Commander
US Army Armor Center
ATTN: ATZK-CD
Fort Knox, KY 40121

Aerodyne Research Inc.
ATTN: Dr. John Ebersole
Bedford Research Park
Crosby Drive
Bedford, MA 01730

Commander
Air Force Geophysical Laboratory
ATTN: OPI (Dr. R.A. McClatchey)
Hanscom AFB, MA 01731

Commander
Air Force Geophysical Laboratory
ATTN: OPI (Dr. R. Fenn)
Hanscom AFB, MA 01731

Commander
US Army Ordnance Center and School
ATTN: ATSL-CD
Aberdeen Proving Ground, MD 21005

Commander
US Army Ordnance & Chemical Center
and School
ATTN: ATSL-CLC (Dr. Thomas Welch)
Aberdeen Proving Ground, MD 21005

Commander
US Army Ballistic Rsch Laboratory
ATTN: Dr. Robert Eichelberge
Aberdeen Proving Ground, MD 21005

Commander
US Army Ballistic Rsch Laboratory
ATTN: Mr. Alan Downs
Aberdeen Proving Ground, MD 21005

Commander
US Army Ballistic Rsch Laboratory
ATTN: DRDAR-BLB (Mr. Arthur LaGrange)
Aberdeen Proving Ground, MD 21005

Commander
US Army Ballistic Research Laboratory
ATTN: Mr. Richard McGee
Aberdeen Proving Ground, MD 21005

Project Manager
Smoke/Obscurants
ATTN: DRDPM-SMC (COL H. Shelton)
Aberdeen Proving Ground, MD 21005

Project Manager
Smoke/Obscurants
ATTN: DRDPM-SMC (Dr. T. Van de Wal Jr.)
Aberdeen Proving Ground, MD 21005

Project Manager
Smoke/Obscurants
ATTN: DRDPM-SMC (Mr. G. Bowman)
Aberdeen Proving Ground, MD 21005

Project Manager
Smoke/Obscurants
ATTN: DRDPM-SMC (Mr. J. Steedman)
Aberdeen Proving Ground, MD 21005

Commander
US Army Test & Evaluation Command
ATTN: DRSTE-AD-M (Mr. Warren M. Baily)
Aberdeen Proving Ground, MD 21005

Director
US Army Material Systems Analysis Activity
ATTN: DRXSY-LA (Mr. Paul Frossell)
Aberdeen Proving Ground, MD 21005

Director
US Army Material Systems Analysis Activity
ATTN: DRXSY-LA (Mr. Michael Starks)
Aberdeen Proving Ground, MD 21005

Director
US Army Material Systems Analysis Activity
ATTN: DRXSY-LA (Mr. William Smith)
Aberdeen Proving Ground, MD 21005

Director
US Army Material Systems Analysis Activity
ATTN: DRXSY-LA (Dr. Keats Pullen)
Aberdeen Proving Ground, MD 21005

Director
US Army Material Systems Analysis Activity
ATTN: DRXSY-GI (Mr. Sid Geraud)
Aberdeen Proving Ground, MD 21005

Director
US Army Armament R&D Command
Chemical Systems Laboratory
ATTN: DRDAR-CLB-PS (Dr. Ed Stuebing)
Aberdeen Proving Ground, MD 21010

Director
US Army Armament R&D Command
Chemical Systems Laboratory
ATTN: DRDAR-CLB-PS (Mr. Joseph Vervier)
Aberdeen Proving Ground, MD 21010

Director
US Army Armament R&D Command
Chemical Systems Laboratory
ATTN: DRDAR-CLY-A (Mr. Ron Pennsyle)
Aberdeen Proving Ground, MD 21010

Commander
Harry Diamond Laboratories
ATTN: Dr. William Carter
2800 Powder Mill Road
Adelphi, MD 20783

Commander
Harry Diamond Laboratories
ATTN: DELHD-RAC (Dr. R.G. Humphrey)
2800 Powder Mill Road
Adelphi, MD 20783

Commander
Harry Diamond Laboratories
ATTN: Dr. Ed Brown
2800 Powder Mill Road
Adelphi, MD 20783

Commander
Harry Diamond Laboratories
ATTN: Dr. Stan Kulpa
2800 Powder Mill Road
Adelphi, MD 20783

Commander
ERADCOM
ATTN: DRDEL-AP
2800 Powder Mill Road
Adelphi, MD 20783
2

Commander
ERADCOM
ATTN: DRDEL-CG/DRDEL-DC/DRDEL-CS
2800 Powder Mill Road
Adelphi, MD 20783

Commander
ERADCOM
ATTN: DRDEL-CT
2800 Powder Mill Road
Adelphi, MD 20783

Commander
ERADCOM
ATTN: DRDEL-EA
2800 Powder Mill Road
Adelphi, MD 20783

Commander
ERADCOM
ATTN: DRDEL-PA/DRDEL-ILS/DRDEL-E
2800 Powder Mill Road
Adelphi, MD 20783

Commander
ERADCOM
ATTN: DRDEL-PAO (S. Kimmel)
2800 Powder Mill Road
Adelphi, MD 20783

Commander
ERADCOM
ATTN: DRDEL-PAO (Paul Case)
2800 Powder Mill Road
Adelphi, MD 20783

Commander
HQ, AFSC/DLCAA
ATTN: LTC Glen Warner
Andrews AFB, MD 20334

AFSC
ATTN: WER (Mr. Richard F. Picanso)
Andrews AFB, MD 20334

Commander
Concepts Analysis Agency
ATTN: MOCA-SMC (Hal E. Hock)
8120 Woodmont Ave
Bethesda, MD 20014

Martin Marietta Laboratories
ATTN: Jar Mo Chen
1450 South Rolling Road
Baltimore, MD 21227

Commander
US Army Intelligence Agency
Fort George G. Meade, MD 20755

Director
National Security Agency
ATTN: R52/Woods
Fort George G. Meade, MD 20755

Chief
Intelligence Materiel Dev & Support Ofc
ATTN: DELEW-WL-I
Bldg 4554
Fort George G. Meade, MD 20755

Acquisitions Section, IRDB-D823
Library & Info Service Div, NOAA
6009 Executive Blvd
Rockville, MD 20852

Naval Surface Weapons Center
ATTN: Code WR42 (Dr. Barry Katz)
White Oak Library
Silver Spring, MD 20910

The Environmental Research
Institute of MI
ATTN: IRIA Library
PO Box 8618
Ann Arbor, MI 48107

Science Applications Inc.
ATTN: Dr. Robert E. Meredith
15 Research Drive
PO Box 7329
Ann Arbor, MI 48107

Science Applications Inc.
ATTN: Dr. Robert E. Turner
15 Research Drive
PO Box 7329
Ann Arbor, MI 48107

Commander
US Army Tank-Automative R&D Command
Warren, MI 48090

Dr. A. D. Belmont
Research Division
PO Box 1249
Control Data Corp
Minneapolis, MN 55440

Commander
US Army Aviation Systems Command
St. Louis, MO 63166

Director
Naval Oceanography & Meteorology
NSTL Station
Bay St Louis, MS 39529

Director
US Army Engr Waterways Experiment Sta
ATTN: Library
PO Box 631
Vicksburg, MS 39180

Director
US Army Engr Waterways Experiment Sta
ATTN: WESFT (Dr. Bob Penn)
PO Box 631
Vicksburg, MS 39180

Director
US Army Engr Waterways Experiment Sta
ATTN: WESFT (Mr. Jerry Lundien)
PO Box 631
Vicksburg, MS 39180

US Army Research Office
ATTN: DRXRO-PP
PO Box 12211
Research Triangle Park, NC 27709

US Army Research Office
ATTN: DRXRO-GS (Dr. Arthur V. Dodd)
PO Box 12211
Research Triangle Park, NC 27709

Commander
US Army Cold Regions Rsch & Engr Lab
ATTN: Mr. Roger Berger
Hanover, NH 03755

Commander
US Army Cold Regions Rsch & Engr Lab
ATTN: Mr. George Aitken
Hanover, NH 03755

Commander
US Army Cold Regions Rsch & Engr Lab
ATTN: CRREL-RD (Dr. K.F. Sterrett)
Hanover, NH 03755

Commander
US Army Armament R&D Command
ATTN: DRDAR-TSS (Bldg 59)
Dover, NJ 07801

Commander
US Army Armament R&D Command
ATTN: DRDAR-AC (J. Greenfield)
Dover, NJ 07801

Project Manager
Cannon Artillery Weapons Systems
ATTN: DRCPM-CAWS
Dover, NJ 07801

Project Manager
Cannon Artillery Weapons Systems
ATTN: DRCPM-CAWS-GP (G.H. Waldron)
Dover, NJ 07801

Commander
HQ, US Army Avionics R&D Activity
ATTN: DAVAA-O
Fort Monmouth, NJ 07703

Commander/Director
US Army Combat Surveillance & Target
Acquisition Laboratory
ATTN: DELCS-D
Fort Monmouth, NJ 07703

Director
US Army Electronics Technology &
Devices Laboratory
ATTN: DELET-D
Fort Monmouth, NJ 07703

Commander
US Army Electronic Warfare Laboratory
ATTN: DELEW-D (Mr. George Haber)
Fort Monmouth, NJ 07703

Commander
US Army Night Vision &
Electro-Optics Laboratory
ATTN: DELNV-L (Dr. Rudolf Buser)
Fort Monmouth, NJ 07703

Commander
US Army Night Vision &
Electro-Optics Laboratory
ATTN: DELNV-L (Dr. Robert Rodhe)
Fort Monmouth, NJ 07703

Commander
ERADCOM Technical Support Activity
ATTN: DELSD-L
Fort Monmouth, NJ 07703

Project Manager, FIREFINDER
ATTN: DRCPM-FF
Fort Monmouth, NJ 07703

Project Manager, REMBASS
ATTN: DRCPM-RBS
Fort Monmouth, NJ 07703

Commander
US Army Satellite Comm Agency
ATTN: DRCPM-SC-3
Fort Monmouth, NJ 07703

Commander
ERADCOM Scientific Advisor
ATTN: DRDEL-SA
Fort Monmouth, NJ 07703

Project Manager
Army Tactical Data Systems
ATTN: DRCPM-TDS
Fort Monmouth, NJ 07703

6585 TG/WE
Holloman AFB, NM 88330

AFWL/WE
Kirtland, AFB, NM 87117

AFWL/Technical Library (SUL)
Kirtland AFB, NM 87117

Commander
US Army Test & Evaluation Command
ATTN: STEWS-AD-L
White Sands Missile Range, NM 88002

Chief
US Army Electronics R&D Command
Office of Missile Electronic Warfare
ATTN: DELEW-M-STE (Dr. Steven Kovel)
White Sands Missile Range, NM 88002

US Army Office of the Test Director
Joint Services EO GW CM Test Program
ATTN: DRXDE-TD (Mr. Weldon Findley)
White Sands Missile Range, NM 88002

Commander
TRASANA
ATTN: ATAA-D (Dr. Wilbur Payne)
White Sands Missile Range, NM 88002

Commander
TRASANA
ATTN: ATAA-TDB (Louis Dominquez)
White Sands Missile Range, NM 88002

Commander
TRASANA
ATTN: ATAA-PL (Dolores Anguiano)
White Sands Missile Range, NM 88002

Commander
TRASANA
ATTN: ATAA-TOP (Roger Willis)
White Sands Missile Range, NM 88002

Commander
TRASANA
ATTN: ATAA-TGC (Dr. Alfonso Diaz)
White Sands Missile Range, NM 88002

Commander
TRASANA
ATTN: ATAA-TGA (Mr. Edward Henry)
White Sands Missile Range, NM 88002

Grumman Aerospace Corporation
Research Dept - MS A08-35
ATTN: John E. A. Selby
Bethpage, NY 11714

Rome Air Development Center
ATTN: Documents Library
TSLD (Bette Smith)
Griffiss AFB, NY 13441

Commander
US Army Tropic Test Center
ATTN: STETC-TD (Info Center)
APO New York 09827

Commander
US Army R&D Coordinator
US Embassy, Bonn, Box 165
APO New York 09080

HQ
USAREUR & Seventh Army
APO New York, NY 09403

Air Force Avionics Laboratory
ATTN: AFAL/RWI-3 (Cpt James Pryce)
Wright-Patterson AFB, OH 45433

Air Force Air Systems Laboratory
ATTN: AFAL/RWI-e (Dr. George Mavko)
Wright-Patterson AFB, OH 45433

Commandant
US Army Field Artillery School
ATTN: ATSF-CD-R (Mr. Farmer)
Fort Sill, OK 73503

Commandant
US Army Field Artillery School
ATTN: ATSF-CF-R
Fort Sill, OK 73503

Director CFD
US Army Field Artillery School
ATTN: Met Division
Fort Sill, OK 73503

Commandant
US Army Field Artillery School
ATTN: Morris Swett Library
Fort Sill, OK 73503

Commander
US Army Combined Arms Center
ATTN: ATCA-CAT-V (R. DeKinder, Jr.)
Fort Sill, OK 73503

US Army Field Artillery School
ATTN: ATSF-CD
Fort Sill, OK 73503

Commander
273rd Transportation Company
(Heavy Helicopter)
W44CCQ
ATTN: CW4 J. Kard
Fort Sill, OK 73503

Commander
Naval Air Development Center
ATTN: Code 202 (Mr. Thomas Shopple)
Warminster, PA 18974

University of Texas at El Paso
Electrical Engineering Department
ATTN: Dr. Joseph H. Pierluissi
El Paso, TX 79968

US Army Air Defense School
ATTN: ATSA-CD
Fort Bliss, TX 79916

Commander
3rd Armored Cavalry Regiment
ATTN: AFVF-SO
Fort Bliss, TX 79916

Commander
TRADOC Combined Arms Test Activity
ATTN: ATCAT-OP-Q (Wayland Smith)
Fort Hood, TX 76544

Commander
TRADOC Combined Arms Test Activity
ATTN: Technical Library
Fort Hood, TX 76544

Commander
TRADOC Combined Arms Test Activity
ATTN: ATCAT-SCI (Darrell Collin)
Fort Hood, TX 76544

MAJ Joseph Caruso
HQ, TRADOC Combined Arms Test Activity
ATTN: ATCAT-CA
Fort Hood, TX 76544

Commandant
US Army Air Defense School
ATTN: Mr. Blanchett
Fort Bliss, TX 79916

Commander
US Army Dugway Proving Ground
ATTN: STEDP-MT-DA-L
Dugway, UT 84022

Commander
US Army Dugway Proving Ground
ATTN: STEDP-MT-DA-S (John Treatheway)
Dugway, UT 84022

Commander
US Army Dugway Proving Ground
ATTN: STEDP-MT-DA-M (Paul Carlson)
Dugway, UT 84022

Commander
US Army Dugway Proving Ground
ATTN: STEDP-MT-DA-T (William Peterson)
Dugway, UT 84022

Defense Documentation Center
ATTN: DDC-TCA
Cameron Station Bldg 5
Alexandria, VA 22314
12

Ballistic Missile Defense Program Office
ATTN: DACS-BMT
5001 Eisenhower Avenue
Alexandria, VA 22333

Commander
US Army Materiel Dev & Readiness Command
ATTN: DRCLDC (Mr. James Bender)
5001 Eisenhower Ave
Alexandria, VA 22333

Commander
US Army Materiel Dev & Readiness Command
ATTN: DRCBSI
5001 Eisenhower Ave
Alexandria, VA 22333

Institute for Defense Analysis
ATTN: Mr. Lucian Biberman
Arlington, VA 22202

Institute for Defense Analysis
ATTN: Dr. Robert Roberts
Arlington, VA 22202

Director
ARPA
1400 Wilson Blvd
Arlington, VA 22209

Defense Advanced Rsch Projects Agency
ATTN: Steve Zakanyez
1400 Wilson Blvd
Arlington, VA 22209

Defense Advanced Rsch Projects Agency
ATTN: Dr. Carl Thomas
1400 Wilson Blvd
Arlington, VA 22209

Defense Advanced Rsch Projects Agency
ATTN: Dr. James Tegnelia
1400 Wilson Blvd
Arlington, VA 22209

Commander
US Army Security Agency
ATTN: IARD-MF
Arlington Hall Station
Arlington, VA 22212

USA Intelligence & Security Command
ATTN: E. A. Speakman,
Science Advisor
Arlington Hall Station
Arlington, VA 22212

Commander
US Army Foreign Sci & Tech Center
ATTN: DRXST-IS1
220 7th Street, NE
Charlottesville, VA 22901

Commander
US Army Foreign Sci & Tech Center
ATTN: Dr. Orville Harris
220 7th Street, NE
Charlottesville, VA 22901

Commander
US Army Foreign Sci & Tech Center
ATTN: Dr. Bertram Smith
220 7th Street, NE
Charlottesville, VA 22901

Naval Surface Weapons Center
ATTN: Code G65
Dahlgren, VA 22448

Commander
Operational Test & Evaluation Agency
Columbia Pike Bldg
5600 Columbia Pike
Falls Church, VA 22041

Commander
US Army Night Vision
& Electro-Optics Lab
ATTN: DELNV-D (Mr. John Johnson)
Fort Belvoir, VA 22060

Commander
US Army Night Vision
& Electro-Optics Lab
ATTN: DELNV-VI (Mr. J.R. Moulton)
Fort Belvoir, VA 22060

Commander
US Army Night Vision
& Electro-Optics Lab
ATTN: DELNV-VI (Luanne Overt)
Fort Belvoir, VA 22060

Commander
US Army Night Vision
& Electro-Optics Lab
ATTN: DELNV-VI (Tom Cassidy)
Fort Belvoir, VA 22060

Commander
US Army Night Vision
& Electro-Optics Lab
ATTN: DELNV-VI (Richard Bergemann)
Fort Belvoir, VA 22060

Commander
US Army Night Vision
& Electro-Optics Lab
ATTN: DELNV-VI (Dr. John Ratches)
Fort Belvoir, VA 22060

Commander
US Army Night Vision
& Electro-Optics Lab
ATTN: DELNV-FIR (Fred Petito)
Fort Belvoir, VA 22060

Commander
US Army Engineering Topographic Lab
ATTN: ETL-TD-MB
Fort Belvoir, VA 22060

US Army Engineer School
ATTN: ATSE-CD
Fort Belvoir, VA 22060

Commandant
US Army Engineering Center & School
Directorate of Combat Developments
Fort Belvoir, VA 22060

Commander
US Army Mobility Equip R&D Command
ATTN: DRDME-RT (Mr. Fred Kezer)
Fort Belvoir, VA 22060

Director
Applied Technology Laboratory
ATTN: DAVDL-EU-TSD (Tech Library)
Fort Eustis, VA 23604

Department of the Air Force
OL-C, 5WW
Fort Monroe, VA 23651

Commander
HQ, TRADOC
ATTN: ATCD-PM
Fort Monroe, VA 23651

Commander
US Army Training & Doctrine Command
Fort Monroe, VA 23651

Commander
US Army Training & Doctrine Command
ATTN: ATCD-IE-R (Mr. Dave Ingram)
Fort Monroe, VA 23651

Commander
US Army Training & Doctrine Command
ATTN: ATCD-STE
Fort Monroe, VA 23651

Commander
US Army Training & Doctrine Command
ATTN: ATCD-CF (Chris O'Conner)
Fort Monroe, VA 23651

Commander
US Army Training & Doctrine Command
ATTN: ATCD-AN-TD (Seymour Goldbert)
Fort Monroe, VA 23651

Commander
US Army Training & Doctrine Command
ATTN: ATCD-TA (M. P. Pastel)
Fort Monroe, VA 23651

Commander
US Army Training & Doctrine Command
ATTN: Tech Library
Fort Monroe, VA 23651

Department of the Air Force
5WW/DN
Langley AFB, VA 23665

Commander
US Army INSCOM/QRC
6845 Elm Street - S407
McLean, VA 22101

MITRE Corporation
ATTN: Robert Finkelstein
1820 Dolley Madison Blvd
McLean, VA 22101

Science Applications, Inc.
8400 Westpark Drive
ATTN: Dr. John E. Cockayne
McLean, VA 22101

Director
Development Center MCDEC
ATTN: Firepower Division
Quantico, VA 22134

US Army Nuclear & Chemical Agency
ATTN: MONA-WE (Dr. Jack Berberet)
7500 Backlick Road
Springfield, VA 22150

Director
US Army Signals Warfare Laboratory
ATTN: DELSW-OS (Dr. R. Burkhardt)
Vint Hill Farms Station
Warrenton, VA 22186

Commander
US Army Cold Regions Test Center
ATTN: STECR-OP-PM
APO Seattle, WA 98733

Effects Technology Inc.
ATTN: Jack Carlyle
5383 Hollister Avenue
Santa Barbara, CA 93111

Raytheon Company
Electro-Optics Department
ATTN: Dr. Charles M. Sonnenschein
Boston Post Road
Wayland, MA 01778

Norden Systems
ATTN: Estelle Thurman, Librarian
Norwalk, CT 06856

MIT Lincoln Laboratory
ATTN: Dr. T. Goblick, D-447
PO Box 73
Lexington, MA 02173

Commander/Director
US Army Combat Surveillance & Target
Acquisition Laboratory
ATTN: DELCS-R (Mr. David Longinotti)
Fort Monmouth, NJ 07703

General Research Corporation
ATTN: Dr. Ralph Zirkind
7655 Old Springhouse Road
McLean, VA 22101

Commander
MIRADCOM
ATTN: DRDMI-TE (Mr. W. J. Lindberg)
Huntsville, AL 35807

Teledyne Brown Engineering
ATTN: Bruce Tully, Mail Stop 19
Cummings Research Park
Huntsville, AL 35807

Applied Physics Laboratory
John Hopkins University
ATTN: Dr. Michael Lun
John Hopkins Road
Laurell, MD 20810

ATMOSPHERIC SCIENCES RESEARCH PAPERS

1. Lindberg, J.D., "An Improvement to a Method for Measuring the Absorption Coefficient of Atmospheric Dust and other Strongly Absorbing Powders," ECOM-5565, July 1975.
2. Avara, Elton, P., "Mesoscale Wind Shears Derived from Thermal Winds," ECOM-5566, July 1975.
3. Gomez, Richard B., and Joseph H. Pierluissi, "Incomplete Gamma Function Approximation for King's Strong-Line Transmittance Model," ECOM-5567, July 1975.
4. Blanco, A.J., and B.F. Engebos, "Ballistic Wind Weighting Functions for Tank Projectiles," ECOM-5568, August 1975.
5. Taylor, Fredrick J., Jack Smith, and Thomas H. Pries, "Crosswind Measurements through Pattern Recognition Techniques," ECOM-5569, July 1975.
6. Walters, D.L., "Crosswind Weighting Functions for Direct-Fire Projectiles," ECOM 5570, August 1975.
7. Duncan, Louis D., "An Improved Algorithm for the Iterated Minimal Information Solution for Remote Sounding of Temperature," ECOM-5571, August 1975.
8. Robbiani, Raymond L., "Tactical Field Demonstration of Mobile Weather Radar Set AN TPS-41 at Fort Rucker, Alabama," ECOM-5572, August 1975.
9. Miers, B., G. Blackman, D. Langer, and N. Lorimer, "Analysis of SMS GOES Film Data," ECOM-5573, September 1975.
10. Manquero, Carlos, Louis Duncan, and Rufus Bruce, "An Indication from Satellite Measurements of Atmospheric CO2 Variability," ECOM-5574, September 1975.
11. Petracca, Carmine, and James D. Landberg, "Installation and Operation of an Atmospheric Particulate Collector," ECOM-5575, September 1975.
12. Avara, Elton P., and George Alexander, "Empirical Investigation of Three Iterative Methods for Inverting the Radiative Transfer Equation," ECOM-5576, October 1975.
13. Alexander, George D., "A Digital Data Acquisition Interface for the SMS Direct Readout Ground Station Concept and Preliminary Design," ECOM 5577, October 1975.
14. Cantor, Israel, "Enhancement of Point Source Thermal Radiation Under Clouds in a Nonattenuating Medium," ECOM-5578, October 1975.
15. Norton, Colburn, and Glenn Hoidale, "The Diurnal Variation of Mixing Height by Month over White Sands Missile Range, N.M," ECOM-5579, November 1975.
16. Avara, Elton P., "On the Spectrum Analysis of Binary Data," ECOM-5580, November 1975.
17. Taylor, Fredrick J., Thomas H. Pries, and Chao-Huan Huang, "Optimal Wind Velocity Estimation," ECOM-5581, December 1975.
18. Avara, Elton P., "Some Effects of Autocorrelated and Cross-Correlated Noise on the Analysis of Variance," ECOM-5582, December 1975.
19. Gillespie, Patti S., R.L. Armstrong, and Kenneth O. White, "The Spectral Characteristics and Atmospheric CO2 Absorption of the Ho:YLF Laser at 2.05μm," ECOM-5583, December 1975.
20. Novlan, David J. "An Empirical Method of Forecasting Thunderstorms for the White Sands Missile Range," ECOM-5584, February 1976.
21. Avara, Elton P., "Randomization Effects in Hypothesis Testing with Autocorrelated Noise," ECOM-5585, February 1976.
22. Watkins, Wendell R., "Improvements in Long Path Absorption Cell Measurement," ECOM-5586, March 1976.
23. Thomas, Joe, George D. Alexander, and Marvin Dubbin, "SATTEL An Army Dedicated Meteorological Telemetry System," ECOM-5587, March 1976.
24. Kennedy, Bruce W., and Delbert Bynum, "Army User Test Program for the RDT&E-XM-75 Meteorological Rocket," ECOM-5588, April 1976.

25. Barnett, Kenneth M., "A Description of the Artillery Meteorological Comparisons at White Sands Missle Range, October 1974 - December 1974 ('PASS' - Prototype Artillery [Meteorological] Subsystem)," ECOM-5589, April 1976.
26. Miller, Walter B., "Preliminary Analysis of Fall-of-Shot From Project 'PASS'," ECOM-5590, April 1976.
27. Avara, Elton P., "Error Analysis of Minimum Information and Smith's Direct Methods for Inverting the Radiative Transfer Equation," ECOM-5591, April 1976.
28. Yee, Young P., James D. Horn, and George Alexander, "Synoptic Thermal Wind Calculations from Radiosonde Observations Over the Southwestern United States," ECOM-5592, May 1976.
29. Duncan, Louis D., and Mary Ann Seagraves, "Applications of Empirical Corrections to NOAA-4 VTPR Observations," ECOM-5593, May 1976.
30. Miers, Bruce T., and Steve Weaver, "Applications of Meterological Satellite Data to Weather Sensitive Army Operations,"ECOM-5594, May 1976.
31. Sharenow, Moses, "Redesign and Improvement of Balloon ML-566," ECOM-5595, June, 1976.
32. Hansen, Frank V., "The Depth of the Surface Boundary Layer," ECOM-5596, June 1976.
33. Pinnick, R.G., and E.B. Stenmark, "Response Calculations for a Commercial Light-Scattering Aerosol Counter," ECOM-5597, July 1976.
34. Mason, J., and G.B. Hoidale, "Visibility as an Estimator of Infrared Transmittance," ECOM-5598, July 1976.
35. Bruce, Rufus E., Louis D. Duncan, and Joseph H. Pierluissi, "Experimental Study of the Relationship Between Radiosonde Temperatures and Radiometric-Area Temperatures," ECOM-5599, August 1976.
36. Duncan, Louis D., "Stratospheric Wind Shear Computed from Satellite Thermal Sounder Measurements," ECOM-5800, September 1976.
37. Taylor, F., P. Mohan, P. Joseph and T. Pries, "An All Digital Automated Wind Measurement System," ECOM-5801, September 1976.
38. Bruce, Charles, "Development of Spectrophones for CW and Pulsed Radiation Sources," ECOM-5802, September 1976.
39. Duncan, Louis D., and Mary Ann Seagraves,"Another Method for Estimating Clear Column Radiances," ECOM-5803, October 1976.
40. Blanco, Abel J., and Larry E. Taylor, "Artillery Meteorological Analysis of Project Pass," ECOM-5804, October 1976.
41. Miller, Walter, and Bernard Engebos," A Mathematical Structure for Refinement of Sound Ranging Estimates," ECOM-5805, November, 1976.
42. Gillespie, James B., and James D. Lindberg, "A Method to Obtain Diffuse Reflectance Measurements from 1.0 to 3.0 μm Using a Cary 17I Spectrophotometer," ECOM-5806, November 1976.
43. Rubio, Roberto, and Robert O. Olsen,"A Study of the Effects of Temperature Variations on Radio Wave Absorption,"ECOM-5807, November 1976.
44. Ballard, Harold N., "Temperature Measurements in the Stratosphere from Balloon-Borne Instrument Platforms, 1968-1975," ECOM-5808, December 1976.
45. Monahan, H.H., "An Approach to the Short-Range Prediction of Early Morning Radiation Fog," ECOM-5809, January 1977.
46. Engebos, Bernard Francis, "Introduction to Multiple State Multiple Action Decision Theory and Its Relation to Mixing Structures," ECOM-5810, January 1977.
47. Low, Richard D.H.,"Effects of Cloud Particles on Remote Sensing from Space in the 10-Micrometer Infrared Region," ECOM-5811, January 1977.
48 Bonner, Robert S., and R. Newton, "Application of the AN/GVS-5 Laser Rangefinder to Cloud Base Height Measurements," ECOM-5812, February 1977.
49. Rubio, Roberto, "Lidar Detection of Subvisible Reentry Vehicle Erosive Atmospheric Material," ECOM-5813, March 1977.
50. Low, Richard D.H., and J.D. Horn, "Mesoscale Determination of Cloud-Top Height: Problems and Solutions," ECOM-5814, March 1977.

51. Duncan, Louis D., and Mary Ann Seagraves,"Evaluation of the NOAA-4 VTPR Thermal Winds for Nuclear Fallout Predictions," ECOM-5815, March 1977.
52. Randhawa, Jagir S., M. Izquierdo, Carlos McDonald and Zvi Salpeter, "Stratospheric Ozone Density as Measured by a Chemiluminescent Sensor During the Stratcom VI-A Flight," ECOM-5816, April 1977.
53. Rubio, Roberto, and Mike Izquierdo, "Measurements of Net Atmospheric Irradiance in the 0.7- to 2.8-Micrometer Infrared Region," ECOM-5817, May 1977.
54. Ballard, Harold N., Jose M. Serna, and Frank P. Hudson Consultant for Chemical Kinetics, "Calculation of Selected Atmospheric Composition Parameters for the Mid-Latitude, September Stratosphere," ECOM-5818, May 1977.
55. Mitchell, J.D., R.S. Sagar, and R.O. Olsen, "Positive Ions in the Middle Atmosphere During Sunrise Conditions," ECOM-5819, May 1977.
56. White, Kenneth O., Wendell R. Watkins, Stuart A. Schleusener, and Ronald L. Johnson, "Solid-State Laser Wavelength Identification Using a Reference Absorber," ECOM-5820, June 1977.
57. Watkins, Wendell R., and Richard G. Dixon, "Automation of Long-Path Absorption Cell Measurements," ECOM-5821, June 1977.
58. Taylor, S.E., J.M. Davis, and J.B. Mason, "Analysis of Observed Soil Skin Moisture Effects on Reflectance," ECOM-5822, June 1977.
59. Duncan, Louis D. and Mary Ann Seagraves, "Fallout Predictions Computed from Satellite Derived Winds," ECOM-5823. June 1977.
60. Snider, D.E., D.G. Murcray, F.H. Murcray, and W.J. Williams, "Investigation of High-Altitude Enhanced Infrared Backround Emissions" (U), SECRET, ECOM-5824, June 1977.
61. Dubbin, Marvin H. and Dennis Hall, "Synchronous Meteorlogical Satellite Direct Readout Ground System Digital Video Electronics," ECOM-5825, June 1977.
62. Miller, W., and B. Engebos, "A Preliminary Analysis of Two Sound Ranging Algorithms," ECOM-5826, July 1977.
63. Kennedy, Bruce W., and James K. Luers, "Ballistic Sphere Techniques for Measuring Atomspheric Parameters," ECOM-5827, July 1977.
64. Duncan, Louis D., "Zenith Angle Variation of Satellite Thermal Sounder Measurements," ECOM-5828, August 1977.
65. Hansen, Frank V., "The Critical Richardson Number," ECOM-5829, September 1977.
66. Ballard, Harold N., and Frank P. Hudson (Compilers), "Stratospheric Composition Balloon-Borne Experiment," ECOM-5830, October 1977.
67. Barr, William C., and Arnold C. Peterson, "Wind Measuring Accuracy Test of Meteorological Systems," ECOM-5831, November 1977.
68. Ethridge, G.A. and F.V. Hansen, "Atmospheric Diffusion: Similarity Theory and Empirical Derivations for Use in Boundary Layer Diffusion Problems," ECOM-5832, November 1977.
69. Low, Richard D.H., "The Internal Cloud Radiation Field and a Technique for Determining Cloud Blackness," ECOM-5833, December 1977.
70. Watkins, Wendell R., Kenneth O. White, Charles W. Bruce, Donald L. Walters, and James D. Lindberg, "Measurements Required for Prediction of High Energy Laser Transmission," ECOM-5834, December 1977.
71. Rubio, Robert, "Investigation of Abrupt Decreases in Atmospherically Backscattered Laser Energy," ECOM-5835, December 1977.
72. Monahan, H.H. and R.M. Cionco, "An Interpretative Review of Existing Capabilities for Measuring and Forecasting Selected Weather Variables (Emphasizing Remote Means)," ASL-TR-0001, January 1978.
73. Heaps, Melvin G., "The 1979 Solar Eclipse and Validation of D-Region Models," ASL-TR-0002. March 1978.

74. Jennings, S.G., and J.B. Gillespie, "M.I.E. Theory Sensitivity Studies - The Effects of Aerosol Complex Refractive Index and Size Distribution Variations on Extinction and Absorption Coefficients Part II: Analysis of the Computational Results," ASL-TR-0003, March 1978.
75. White, Kenneth O. et al, "Water Vapor Continuum Absorption in the 3.5μm to 4.0μm Region," ASL-TR-0004, March 1978.
76. Olsen, Robert O., and Bruce W. Kennedy, "ABRES Pretest Atmospheric Measurements," ASL-TR-0005, April 1978.
77. Ballard, Harold N., Jose M. Serna, and Frank P. Hudson, "Calculation of Atmospheric Composition in the High Latitude September Stratosphere," ASL-TR-0006, May 1978.
78. Watkins, Wendell R. et al, "Water Vapor Absorption Coefficients at HF Laser Wavelengths," ASL-TR-0007, May 1978.
79. Hansen, Frank V., "The Growth and Prediction of Nocturnal Inversions," ASL-TR-0008, May 1978.
80. Samuel, Christine, Charles Bruce, and Ralph Brewer, "Spectrophone Analysis of Gas Samples Obtained at Field Site," ASL-TR-0009, June 1978.
81. Pinnick, R.G. et al., "Vertical Structure in Atmospheric Fog and Haze and its Effects on IR Extinction," ASL-TR-0010, July 1978.
82. Low, Richard D.H., Louis D. Duncan, and Richard B. Gomez, "The Microphysical Basis of Fog Optical Characterization," ASL-TR-0011, August 1978.
83. Heaps, Melvin G., "The Effect of a Solar Proton Event on the Minor Neutral Constituents of the Summer Polar Mesosphere," ASL-TR-0012, August 1978.
84. Mason, James B., "Light Attenuation in Falling Snow," ASL-TR-0013, August 1978.
85. Blanco, Abel J., "Long-Range Artillery Sound Ranging: "PASS" Meteorological Application," ASL-TR-0014, September 1978.
86. Heaps, M.G., and F.E. Niles, "Modeling the Ion Chemistry of the D-Region: A case Study Based Upon the 1966 Total Solar Eclipse," ASL-TR-0015, September 1978.
87. Jennings, S.G., and R.G. Pinnick, "Effects of Particulate Complex Refractive Index and Particle Size Distribution Variations on Atmospheric Extinction and Absorption for Visible Through Middle-Infrared Wavelengths," ASL-TR-0016, September 1978.
88. Watkins, Wendell R., Kenneth O. White, Lanny R. Bower, and Brian Z. Sojka, " Pressure Dependence of the Water Vapor Continuum Absorption in the 3.5- to 4.0-Micrometer Region," ASL-TR-0017, September 1978.
89. Miller, W.B., and B.F. Engebos, "Behavior of Four Sound Ranging Techniques in an Idealized Physical Enviroment," ASL-TR-0018, September 1978.
90. Gomez, Richard G., "Effectiveness Studies of the CBU-88/B Bomb, Cluster, Smoke Weapon" (U), CONFIDENTIAL ASL-TR-0019, September 1978.
91. Miller, August, Richard C. Shirkey, and Mary Ann Seagraves, "Calculation of Thermal Emission from Aerosols Using the Doubling Technique," ASL-TR-0020, November, 1978.
92. Lindberg, James D. et al., "Measured Effects of Battlefield Dust and Smoke on Visible, Infrared, and Millimeter Wavelengths Propagation: A Preliminary Report on Dusty Infrared Test-I (DIRT-I)," ASL-TR-0021, January 1979.
93. Kennedy, Bruce W., Arthur Kinghorn, and B.R. Hixon, "Engineering Flight Tests of Range Meteorological Sounding System Radiosonde," ASL-TR-0022, February 1979.
94. Rubio, Roberto, and Don Hoock, "Microwave Effective Earth Radius Factor Variability at Wiesbaden and Balboa," ASL-TR-0023, February 1979.
95. Low, Richard D.H., "A Theoretical Investigation of Cloud/Fog Optical Properties and Their Spectral Correlations," ASL-TR-0024, February 1979.

96. Pinnick, R.G., and H.J. Auvermann, "Response Characteristics of Knollenberg Light-Scattering Aerosol Counters," ASL-TR-0025, February 1979.
97. Heaps, Melvin G., Robert O. Olsen, and Warren W. Berning, "Solar Eclipse 1979, Atmospheric Sciences Laboratory Program Overview," ASL-TR-0026 February 1979.
98. Blanco, Abel J., "Long-Range Artillery Sound Ranging: 'PASS' GR-8 Sound Ranging Data," ASL-TR-0027, March 1979.
99. Kennedy, Bruce W., and Jose M. Serna, "Meteorological Rocket Network System Reliability," ASL-TR-0028, March 1979.
100. Swingle, Donald M., "Effects of Arrival Time Errors in Weighted Range Equation Solutions for Linear Base Sound Ranging," ASL-TR-0029, April 1979.
101. Umstead, Robert K., Ricardo Pena, and Frank V. Hansen, "KWIK: An Algorithm for Calculating Munition Expenditures for Smoke Screening/Obscuration in Tactical Situations," ASL-TR-0030, April 1979.
102. D'Arcy, Edward M., "Accuracy Validation of the Modified Nike Hercules Radar," ASL-TR-0031, May 1979.
103. Rodriguez, Ruben, "Evaluation of the Passive Remote Crosswind Sensor," ASL-TR-0032, May 1979.
104. Barber, T.L., and R. Rodgriquez, "Transit Time Lidar Measurement of Near-Surface Winds in the Atmosphere," ASL-TR-0033, May 1979.
105. Low, Richard D.H., Louis D. Duncan, and Y.Y. Roger R. Hsiao, "Microphysical and Optical Properties of California Coastal Fogs at Fort Ord," ASL-TR-0034, June 1979.
106. Rodriguez, Ruben, and William J. Vechione, "Evaluation of the Saturation Resistant Crosswind Sensor," ASL-TR-0035, July 1979.
107. Ohmstede, William D., "The Dynamics of Material Layers," ASL-TR-0036, July 1979.
108. Pinnick, R.G., S.G. Jennings, Petr Chylek, and H.J. Auvermann "Relationships between IR Extinction, Absorption, and Liquid Water Content of Fogs," ASL-TR-0037, August 1979.
109. Rodriguez, Ruben, and William J. Vechione, "Performance Evaluation of the Optical Crosswind Profiler," ASL-TR-0038, August 1979.
110. Miers, Bruce T., "Precipitation Estimation Using Satellite Data" ASL-TR-0039, September 1979.
111. Dickson, David H., and Charles M. Sonnenschein, "Helicopter Remote Wind Sensor System Description," ASL-TR-0040, September 1979.
112. Heaps, Melvin, G., and Joseph M. Heimerl, "Validation of the Dairchem Code, I: Quiet Midlatitude Conditions," ASL-TR-0041, September 1979.
113. Bonner, Robert S., and William J. Lentz, "The Visioceilometer: A Portable Cloud Height and Visibility Indicator," ASL-TR-0042, October 1979.
114. Cohn, Stephen L., "The Role of Atmospheric Sulfates in Battlefield Obscurations," ASL-TR-0043, October 1979.
115. Fawbush, E.J. et al, "Characterization of Atmospheric Conditions at the High Energy Laser System Test Facility (HELSTF), White Sands Missile Range, New Mexico, Part I, 24 March to 8 April 1977," ASL-TR-0044, November 1979
116. Barber, Ted L., "Short-Time Mass Variation in Natural Atmospheric Dust," ASL-TR-0045, November 1979
117. Low, Richard D.H., "Fog Evolution in the Visible and Infrared Spectral Regions and its Meaning in Optical Modeling," ASL-TR-0046, December 1979

• U.S. GOVERNMENT PRINTING OFFICE: 1980 — 677-119/50